Guéra, A., Gasulla, F. and Barreno, E. (2016) 'Formation of photosystem II reaction centers that work as energy sinks in lichen symbiotic Trebouxiophyceae microalgae', *Photosynthesis research*, 128(1), pp. 15–33. doi:10.1007/s11120-015-0196-8

(Article begins on next page)

Formation of photosystem II reaction centers that work as energy sinks in lichen symbiotic Trebouxiophyceae microalgae

Alfredo Guéra[1] · Francisco Gasulla[1,2] · Eva Barreno[2]

Received: 24 March 2015 / Accepted: 8 October 2015

Abstract Lichens are poikilohydric symbiotic organisms that can survive in the absence of water. Photosynthesis must be highly regulated in these organisms, which live under continuous desiccation-rehydration cycles, to avoid photooxidative damage. Analysis of chlorophyll *a* fluorescence induction curves in the lichen microalgae of the Trebouxiophyceae *Asterochloris erici* and in *Trebouxia jamesii* (TR1) and *Trebouxia* sp. (TR9) phycobionts, isolated from the lichen *Ramalina farinacea*, shows differences with higher plants. In the presence of the photosynthetic electron transport inhibitor DCMU, the kinetics of Q_A reduction is related to variable fluorescence by a sigmoidal function that approaches a horizontal asymptote. An excellent fit to these curves was obtained by applying a model based on the following assumptions: (1) after closure, the reaction centers (RCs) can be converted into "energy sink" centers (sRCs); (2) the probability of energy leaving the sRCs is very low or zero and (3) energy is not transferred from the antenna of PSII units with sRCs to other PSII units. The formation of sRCs units is also induced by repetitive light saturating pulses or at the transition from dark to light and probably requires the accumulation of reduced Q_A, as well as structural changes in the reaction centers of PSII. This type of energy sink would provide a very efficient way to protect symbiotic microalgae against abrupt changes in light intensity.

Keywords *Asterochloris erici* · Chlorophyll *a* fluorescence · Energy sinks · Fluorescence transient · PSII reaction center · *Trebouxia*

Abbreviations

A	Antenna
b	Photosystem II reaction center
B_t	Fraction of closed PSII reaction centers at time *t*
Chyp	Constant that determines the degree of curvature of fluorescence induction curves
cl	Closed RC
DCMU	3-(3′,4′-dichlorophenyl)-1,1-dimethylurea
E	Energy influx
F_o	Minimal Chl *a* fluorescence intensity in dark-adapted samples
F_m	Maximal Chl *a* fluorescence intensity in dark-adapted samples
F_v	Maximum variable Chl *a* fluorescence ($F_v = F_m - F_o$)
F_v/F_m	An estimate of the maximal quantum yield of PSII photochemistry
F_t	Fluorescence intensity at time *t* during exposure of samples to light
φ_{PSII}	Effective quantum efficiency of PSII photochemistry
J	Light absorption flux per antenna complex or reaction center
K	Rate constant for the transformation of closed centers to energy sink centers
op	Open RC

✉ Alfredo Guéra
alfredo.guera@uah.es

[1] Departamento de Ciencias de la Vida, Universidad de Alcalá, Edificio de Ciencias, Campus externo, 28871 Alcalá de Henares, Madrid, Spain

[2] Botánica, ICBIBE, Facultad de Ciencias Biológicas, Universitat de València, C/Dr. Moliner 50, 46100 Burjassot, Valencia, Spain

NPQ	Non-photochemical quenching of excited state of Chl *a*
OKJIP	Reference to the typical shape of a fluorescence induction curve (O, origin; K, J, I, three inflection points that appear successively in the induction curve; P, peak)
PQ	Plastoquinone
PSI	Photosystem I
P700	Reaction center of the PSI
PSII	Photosystem II
$p_{2,2}$	Probability of excitation energy transfer between two different antenna systems
$p_{2,b}$	Probability of excitation energy transfer between the antenna and P680
Phe	Pheophytin
p_{2G}	Global probability for excitation energy transfer ("exciton" transfer) from one PSII unit to another
RC	Reaction center
s	Energy sink
ROS	Reactive oxygen species
S_m	Complementary area of the fluorescence transient
S_t	Complementary area of the fluorescence transient at time t
V_t	Relative variable fluorescence at time t ($V_t = F_t - F_o/F_m - F_o$)

Introduction

Lichens are symbiotic associations (holobionts) established between fungi (mycobionts) and certain groups of cyanobacteria (cyanobionts) or unicellular green algae (phycobionts) (Margulis and Barreno 2003). Similar to plants, all lichens carry out oxygenic photosynthesis. They are poikilohydric organisms, such that their water content is mainly determined by the availability of water in the environment. The vast majority of lichens are desiccation-tolerant, surviving in a state of suspended animation until water becomes available, which allows them to resume normal metabolism (Rundel 1988; Fos et al. 1999; Jensen et al. 1999). In the hydrated state, exposure to intense light produces photoinhibition; however, under drought conditions, lichens seem to tolerate high light levels (Tuba et al. 1996; Jensen et al. 1999; Bukhow and Carpentier 2004; Barták et al. 2005; Kopecky et al. 2005; Kranner et al. 2005). Alternative mechanisms of energy dissipation have been described in mosses and lichens, in which new quenching centers appear to be functional during desiccation (Heber et al. 2006; Kranner et al. 2003; Heber et al. 2007; Veerman et al. 2007; Heber 2008; Gasulla et al. 2009; Fernández-Marín et al. 2010). According to Bilger et al. (1989), desiccation in green algal symbionts induces a functional interruption of excitation energy transfer between the light harvesting chlorophyll (Chl) *a*/*b* pigment complex and photosystem II (PSII), implying a light-independent mechanism as a direct effector. In bryophytes and lichens, an alternative quencher of chlorophyll fluorescence, characterized by a long-wavelength (740 nm) emission, was detected. Veerman et al. (2007), employing steady-state, low-temperature, and time-resolved chlorophyll fluorescence spectroscopy, provided evidence of a pigment molecule energetically coupled to PSII having an emission band at 740 nm that dominates fluorescence decay in the lichen *Parmelia sulcata* under desiccation. The presence of this quencher has been also detected (Komura et al. 2010) by sub-picosecond fluorescence spectroscopy in the dried state of the lichen *Physciella melanchla*, which contains the phycobiont *Trebouxia* sp. Komura et al. (2010) proposed the operation of a new type of strong quenching operating in dried lichens, probably associated with the antenna of PSII. Slavov et al. (2013) after an ultrafast fluorescence spectroscopy study in *Parmelia sulcata* and kinetic target analysis suggested that two mechanisms are implied in photoprotection during desiccation. The first proposed mechanism is a direct quenching of PSII by the formation of a fluorescent (maximal emission at 740 nm) chlorophyll–chlorophyll charge-transfer state. The second mechanism, according to Slavov et al. (2013), involves a spillover (energy transfer) from PSII to PSI facilitated by a rearrangement of thylakoid membranes during desiccation, which would bring PSII and PSI units into direct contact.

Heber et al. (2007) offered additional evidence for alternative mechanisms, identifying in dehydrated mosses and lichen a fluorescence quenching mechanism that is independent of light activation. Heber and co-workers (Heber et al. 2007, 2011; Heber 2008) subsequently offered convincing proof for the existence of alternative pathways for the dissipation of light energy. In lichens subjected to drying, chlorophyll fluorescence decreases and the stable light-dependent charge separation in the RCs of the photosynthetic apparatus is lost. The removal of structural water is thought to produce a conformational change, such that energy is redirected to alternative sinks where the absorbed light energy is very rapidly (within a picosecond or a few femtoseconds) converted into heat, thus depriving functional RCs of energy and protecting them against photoinactivation (Komura et al. 2010; Heber et al. 2011).

Less is known about the protection mechanisms of the photosynthetic machinery of lichens under hydrated conditions. Usually, the duration of the hydrated state is short and the water content of the thallus is constantly changing,

as it equilibrates with the water potential of the surrounding atmosphere. Lichen growth depends on the photobionts photosynthetic rate and this is dependent on the lichen water status (Green et al. 2008). The recovery of photosynthesis after desiccation also needs a period that can take from minutes to hours (Kranner et al. 2003) and high water content causes a depression of photosynthesis by increased thallus resistance for CO_2 diffusion (Palmqvist et al. 2008 and references therein). These circumstances allow light intensities to often exceed those that saturate photosynthesis, therefore facilitating the formation of reactive oxygen species (ROS). The xanthophyll cycle and the formation of non-photochemical quenching of the excited state of Chl (NPQ) have been considered the main way that most lichens dissipate excess light energy in the hydrated state (Kranner et al. 2005; Heber et al. 2006). A role of state transitions to adjust the input of energy between PSII and PSI has been described for cyanobacteria (Allen et al. 1989) or the free living microalga *Chlamydomonas* (Lemeille and Rochaix 2010). Slavov et al. (2013) found that the 740 nm fluorescence band, which is predominant in desiccated lichens, is also present in hydrated samples of *Parmelia* and they propose that it represents a chlorophyll–chlorophyll charge transfer state whose formation provides an efficient quenching mechanism. Recently, Treves et al. (2013) described a new species of *Chlorella* (*C. ohadii*, Trebouxiophyceae) with a remarkable resistance to photoinhibition in the hydrated state.

Light energy absorbed by chlorophyll molecules is either used in photosynthesis, dissipated as heat, or re-emitted as fluorescence (Krause and Weis 1991; Strasser et al. 2000; Govindjee 2004). These three alternatives are competitive; thus a decrease in one leads to an increase in one or both of the others. Hence, changes in photosynthesis and heat dissipation can be investigated by measuring the yield of Chl *a* fluorescence. When photosynthetic cells are illuminated after a dark period, fluorescence emission has a fast rise followed by a slow decreasing phase (Kautsky effect; see Govindjee 1995 for a historical review). During the fast rise (ms-s), Chl *a* fluorescence transient shows several phases or steps, usually termed OJIP, where O is for origin, the first measured minimal level, J and I are intermediate levels, and P is the peak (for a review and discussion, see Stirbet and Govindjee 2012). Many models have been constructed to explain the changes in Chl *a* fluorescence emission (Lázar 1999; Lázar and Schansker 2009; Stirbet and Govindjee 2011, 2012, and references therein). Most of these models, based on the early theory of Duysens and Sweers (1963), assume that when the primary quinone acceptor (Q_A) of the RC of PSII is reduced by photochemical reactions, the corresponding reaction center is closed and the Chl *a* fluorescence of the antenna is high, whereas when Q_A is in the oxidized state, the RC is open and the fluorescence of the antenna is quenched, i.e. it is decreased (Duysens and Sweers 1963; Krause and Weis 1991; Maxwell and Johnson 2000; Govindjee 2004; Strasser et al. 2004; Baker 2008; Stirbet and Govindjee 2012). See chapters in Govindjee et al. (1986) and Papageorgiou and Govindjee (2004) for full understanding of the relation between Chl *a* fluorescence and various photosynthetic reactions.

Searching for the mechanisms of photosynthesis protection in lichen during the hydrated state, we have found, by analysing Chl *a* fluorescence transient in the presence of the electron transport inhibitor DCMU (3-(3′,4′-dichlorophenyl)-1,1-dimethylurea), evidence for the formation of a special kind of reaction centers (RCs) that work as energy sinks (sink reaction centers, sRCs) in Trebouxiophyceae phycobionts. The physiological significance of the formation of sRCS and the possible relationship with the shape of fluorescence induction curves in *Asterochloris erici* and the two *Trebouxia* phycobionts (*T. jamesii* and *T.* sp. TR9), which ever coexist in the lichen *Ramalina farinacea* (Casano et al. 2011) is discussed in this paper. We propose a new alternative mechanism to prevent photooxidative damage in lichen phycobionts based on the transformation of closed RCs in energy sink RCs able to dissipate excess of light energy as heat.

Materials and methods

Biological material

An axenic strain of the lichen phycobiont *A. erici* (Ahmadjian) Skaloud *et* Peksa (SAG 32.85 = UTEX911) was used in this study. Stock cultures of *A. erici* were maintained in 10-ml tubes with 3 × N Bold's basal medium (BBM3N, Bold and Parker 1962) supplemented with 10 g casein hydrolyzate and 20 g glucose per litre (Ahdmajian 1973). TR1 (*Trebouxia jamesii* (Hildreth and Ahmadjian) Gärtner) and TR9 (*Trebouxia* sp.) were isolated in our laboratory (Casano et al. 2011) from a population of the lichen *R. farinacea* (L.) Ach. according to Gasulla et al. (2010). Samples were cultured in liquid or semisolid BBM3N medium in a growth chamber at 15 °C, under a 14-h/10-h light/dark cycle (light intensity: 25 µmol photons m^{-2} s^{-1}). Cell suspensions from *A. erici*, TR1 and TR9 (volume: 1 ml) were removed from 2-week-old stirred cultures and the cell number was counted using a haemocytometer. The final cell density was adjusted, using sterilized medium, to provide 10^6 cells/ml, and sterile cellulose-acetate discs were then inoculated with 50 µl of

this suspension. The discs were then placed in Petri dishes (Goldsmith et al. 1997) on BBM3N agar supplemented with 10 g casein and 20 g glucose per litre. Experiments with algae grown on discs were carried out for 21 days after inoculation. Cultures were maintained at 20 °C under a 12-h photoperiod, with 30 µmol photons m^{-2} s^{-1} of white light. For each experiment, several plates were randomly chosen; every plate contained five cellulose-acetate discs that were also randomly chosen for the different treatments. Each experiment was repeated four to nine times starting from new stock material, using fresh new cultures, dishes and plates.

Chlorophyll a fluorescence measurements

Chl *a* fluorescence was measured in vivo with a Handy PEA (Plant Efficiency Analyser) fluorometer (Hansatech Instruments Ltd, Norfolk, England) or with a Dual-PAM fluorometer (Walz, Effeltrich, Germany). The discs were placed on a microscope slide wrapped with moist filter paper to keep them in a hydrated state. Samples were kept for 30 min in dark before fluorescence was measured. The fast induction kinetics of Chl *a* fluorescence was monitored using a Handy PEA fluorometer. The excitation light was provided by light-emitting diodes (emission maximum at about 650 nm). The maximal intensity (100 %) was about 3000 µmol photons m^{-2} s^{-1} of PAR (photosynthetic active radiation).

Chlorophyll *a* fluorescence and P700 oxidation kinetics were measured simultaneously under saturating light pulses of 3000 µmol photons m^{-2} s^{-1} using the Dual-PAM 100 fluorometer. The P700 oxidation state was obtained by simultaneous measurements of absorbance changes at 830 and 875 nm, using a beam of modulated light produced by two LED lamps. Chl *a* fluorescence and difference between absorbance changes at 830 and 875 nm were measured by the same photodiode.

DCMU treatments

For DCMU (3-(3′,4′-dichlorophenyl)-1,1-dimethylurea) treatments, samples were soaked in 100 µM DCMU in 0.25 % ethanol for 30–45 min in darkness prior to fluorescence measurement.

Theory

For interpretation of the experimental results, we need to make a theoretical analysis of the fluorescence induction curves in the presence of DCMU. Strasser (1978) postulated that for any possible complex arrangement of interconnected pigment systems, energetic communication, between them, can be expressed by simple equations in terms of energy fluxes between pigment systems (as outfluxes and influxes), rate constants, lifetime of the excited states, probabilities of exciton transfer and exciton density (Strasser 1978, 1981, 1986; Strasser et al. 2004). The total energy influx (E) to a determined pigment system "i" is given as the sum of all energy influxes, $E_i = J_i + \Sigma E_{hi}$, where J_i is the light absorption flux by the pigment system i and E_{hi} is the energy transfer flux from a pigment system "h" to a pigment system "i". The energy outfluxes from "i" to another location (antenna, RC) or form (heat, fluorescence, photochemical energy) "j" is given as $E_i = \Sigma E_{ij}$. The probability p_{ij} that an exciton is transferred or transduced from "i" to "j" is expressed in terms of the energy outflux as: $p_{ij} = E_{ij}/\Sigma E_{ij}$.

In Fig. 1A a bipartite model for PSII is schematically presented. This model assumes that light energy (J) is collected by the antenna pigment–protein complex of PSII (green squares) and then it can be converted to heat or fluorescence (red arrows); or transferred to other antenna units; or channelled to the PSII reaction center (labelled as "b"). Arrows are used to symbolize the energy fluxes. The RCs can be in two possible states: open or closed. In open RCs, all the energy influx is employed in photochemistry: excitation of P_{680} and transfer of one electron to the primary acceptor Phe. The actual process can be more complex with implication of the accessory chlorophyll Chl_{D1}. For a review on the current state of primary photochemistry, see Mamedov et al. (2015). In closed RCs, forward photochemistry is absent but there is only energy cycling. In accordance with the theory of energy fluxes (Strasser 1978, 1981, 1986; Strasser et al. 2004), this model can be defined by the following equation system:

$$\begin{aligned} E_{\mathrm{A}}^{\mathrm{op}} &= J + E_{\mathrm{A}}^{\mathrm{op}} p_{22}(1-B) + B E_2^{\mathrm{cl}} p_{22} \\ E_{\mathrm{A}}^{\mathrm{cl}} &= J + E_{\mathrm{A}}^{\mathrm{op}} p_{22}(1-B) + B E_{\mathrm{A}}^{\mathrm{cl}} p_{22} + E_{\mathrm{b}}^{\mathrm{cl}} p_{\mathrm{b2}}^{\mathrm{cl}} \\ E_{\mathrm{b}}^{\mathrm{op}} &= E_{\mathrm{A}}^{\mathrm{op}} p_{2\mathrm{b}} \\ E_{\mathrm{b}}^{\mathrm{cl}} &= E_{\mathrm{A}}^{\mathrm{cl}} p_{2\mathrm{b}} \end{aligned} \quad (1)$$

where "E_i" is the total energy influx into a given pigment system i; "A" is the pigment–protein antenna component of PSII; "b" is the PSII RC; "op" represents open centers; "p_{22}" is the probability of energy transfer between two PSII antenna systems; "p_{2b}" and "p_{b2}" are the probabilities of energy transfer from antenna to PSII RCs or back transfer from RCs to antenna, respectively; "J" is the light absorption flux by the pigment system; and "B" is the fraction of closed RCs (zero when all RCs are open and 1 when they are all closed). Solving this equation system, and after a series of calculations it can be theoretically deduced (see Strasser et al. 2004; Tsimilli-Michael and Strasser 2013, for a detailed explanation starting from a more complex, but similar, tripartite model) that the

relationship between the proportion of closed reaction centers (B) in the presence of DCMU and the relative variable fluorescence (V), defined as the ratio of the variable fluorescence (F_v) to the maximal variable (F_V) fluorescence ($V \equiv \frac{F_v}{F_V} \equiv \frac{(F-F_o)}{(F_m-F_o)}$) is:

$$V = \frac{B}{1 + Chyp(1-B)}, \quad (2)$$

where $Chyp$ is a constant that determines the curvature of the hyperbola defined by Eq. 2. $Chyp$ is also proportional to the connectivity (probability of energy exchange) between PSII RCs, as $Chyp = (F_V/F_o)\, p_{2G}$, where F_V is the maximal variable fluorescence ($F_m - F_o$), and p_{2G} is the global probability for energy transfer (exciton transfer) from one PSII unit to another (Strasser et al. 2004). Expressions of the form of Eq. 2 are also derived in models that are not based on the theory of energy fluxes, such as those by Joliot and Joliot (1964), Lavergne and Leci (1993) or Lavergne and Trissl (1995); see Joliot and Joliot (2003) for a historical perspective.

Equation 2 is consistent with experimental data obtained in the presence of DCMU, an inhibitor of photosynthetic electron transport in PSII between Q_A and Q_B. Under these conditions the experimental fluorescence induction curve approaches to a hyperbola with a vertical asymptote (Fig. 2, red squares) when plotted in a relative variable fluorescence (V_t) vs. proportion of closed reaction centers (B_t) graph, which degenerates into a straight line (Fig. 2, dashed line) only in the case of lack of connectivity ($p_{2G} = 0$) among different PSII units. An exception is the case of *A. erici* described in this paper, where the V_t versus B_t data of DCMU-treated cells (Fig. 2, blue circles) approach a horizontal (Fig. 2, yellow diamonds) instead of a vertical asymptote.

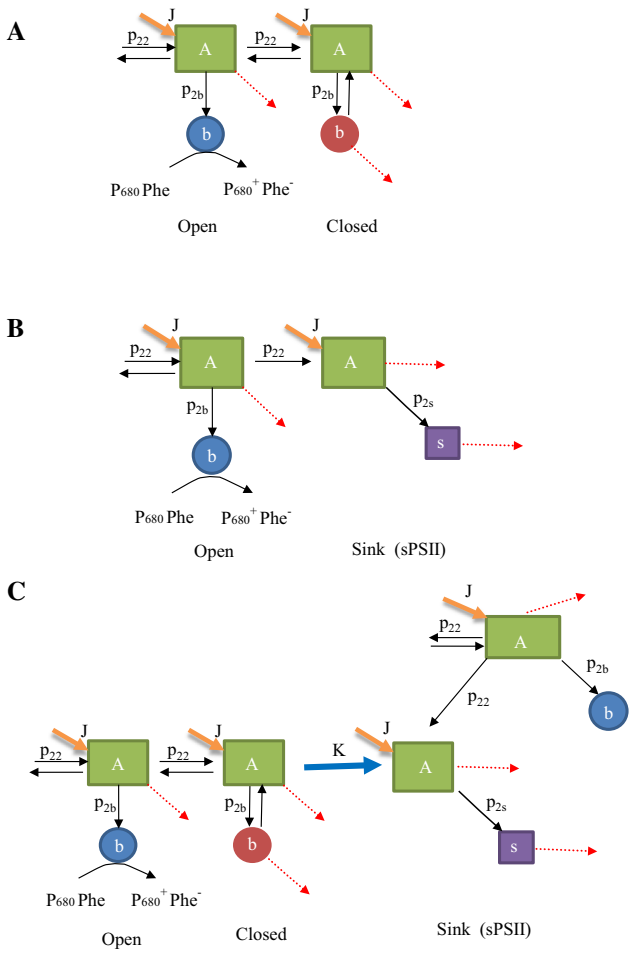

Fig. 1 Bipartite models of energy transfer in photosystem II (PSII). **A** Model for energy transfer in PSII open and closed connected RCs, a simplified version of Strasser's tripartite model (Strasser 1978, 1981, 1986). **B** Model for PSII energy transfer between open RCs (labelled as "b", following Strasser's nomenclature) and RCs that act as energy sinks (sRCS), as described by Eq. 9. **C** Model for PSII energy transfer in *A. erici* as described by Eq. 16, assuming the conversion of closed RCs in sRCs. *Green squares* represent the antenna pigment–protein complexes; *blue circles* the open RCs; *red circles* the closed RCs. *Small purple circles* or *squares* indicate that a conformational or structural change in the RCs has transformed them into sRCs. *Orange arrows* represent the input of light energy (J) reaching the photosystem units. *Black arrows* indicate the transfer of energy between the antenna and the RCs and among different PSII units. *Red discontinuous arrows* represent the losses of energy as heat or fluorescence emission. *Blue arrow* represents the conversion of PSII units with closed RCs in sPSII units (PSII units with sRCs). Here, K is the rate constant for the conversion; p_{22} is the probability of energy transfer between two different antenna complexes; p_{2b} is the probability of energy transfer from an antenna complex to an open or closed RC; and p_{2s} is the probability of energy transfer from the antenna to a sink center. P680 and Phe represent the primary donor and the primary acceptor of PSII, respectively, in the first step of charge separation

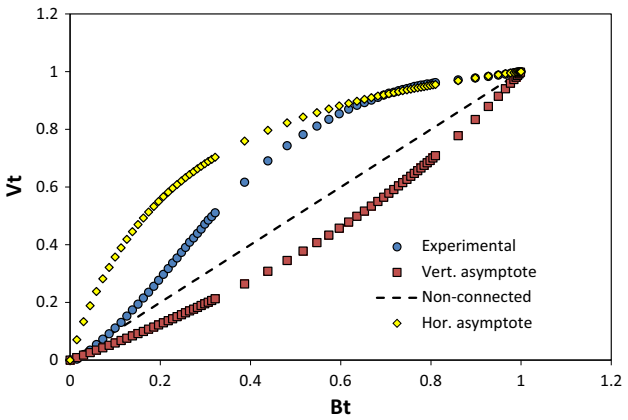

Fig. 2 Relative variable chlorophyll *a* fluorescence (V_t) expressed as a function of the fraction of closed centers (B_t). *Blue circles* experimental data; *dotted line* results expected for disconnected RCs; *red squares* (vertical asymptote), results expected for connected RCs according to models for chlorophyll *a* fluorescence induction, described by Eq. 2; *yellow diamonds* (horizontal asymptote), non-linear regression fitting of experimental data to Eq. 10. The experimental data are the mean from five different samples. See text for further details

An approach to explain the abnormal behaviour of *A. erici* was obtained from the model shown in Fig. 1B. Here, we propose that in *A. erici*, after DCMU treatment, closed RCs are converted into energy sink centers, where most of the energy is dissipated as heat and fluorescence. We assume that the probability of energy leaving the PSII units containing sink RCs, including their antenna, is very low or zero; i.e. these PSII units act, as a whole, as true energy traps. In accordance with the theory of energy fluxes (Strasser 1978, 1981, 1986; Strasser et al. 2004), the equations defining this model are as follows:

$$\begin{aligned} E_{\mathrm{A}}^{\mathrm{op}} &= J + E_{\mathrm{A}}^{\mathrm{op}} p_{22}(1 - B_{\mathrm{s}}) \\ E_{\mathrm{A}}^{\mathrm{s}} &= J + E_{\mathrm{A}}^{\mathrm{op}} p_{22}(1 - B_{\mathrm{s}}) \\ E_{\mathrm{b}} &= E_{\mathrm{A}}^{\mathrm{op}} p_{2\mathrm{b}} \\ E_{\mathrm{s}} &= E_{\mathrm{A}}^{\mathrm{s}} p_{2\mathrm{s}} \end{aligned} \tag{3}$$

where "s" is a "modified" RC acting as an energy sink.

Equation 3 can be easily solved to give the expressions describing the total energy influxes in the antenna and RCs:

$$\begin{aligned} E_{\mathrm{A}}^{\mathrm{op}} &= E_{\mathrm{A}}^{\mathrm{s}} = \frac{J}{1 - p_{22}(1 - B_{\mathrm{s}})} \\ E_{\mathrm{b}} &= \frac{J p_{2\mathrm{b}}}{1 - p_{22}(1 - B_{\mathrm{s}})} \\ E_{\mathrm{s}} &= \frac{J p_{2\mathrm{s}}}{1 - p_{22}(1 - B_{\mathrm{s}})} \end{aligned} \tag{4}$$

For extreme cases in which all centers are open ($E_{\mathrm{A},0}^{\mathrm{op}}$) or are sinks ($E_{\mathrm{A,M}}^{\mathrm{s}}$):

$$\begin{aligned} E_{\mathrm{A},0}^{\mathrm{op}} &= \frac{J}{1 - p_{22}} \\ E_{\mathrm{A,M}}^{\mathrm{s}} &= J \end{aligned} \tag{5}$$

Thus,

$$\begin{aligned} &E_{\mathrm{A}}^{\mathrm{op}} = E_{\mathrm{A},0}^{\mathrm{op}} \frac{1 - p_{22}}{1 - p_{22}(1 - B_{\mathrm{s}})};\ E_{\mathrm{A,tot}}^{\mathrm{op}} = E_{\mathrm{A},0}^{\mathrm{op}} \left(\frac{1 - p_{22}}{1 - p_{22}(1 - B_{\mathrm{s}})} \right)(1 - B_{\mathrm{s}}) \\ &E_{\mathrm{A}}^{\mathrm{s}} = E_{\mathrm{A,max}}^{\mathrm{s}} \frac{1}{1 - p_{22}(1 - B_{\mathrm{s}})};\ E_{\mathrm{A,tot}}^{\mathrm{s}} = E_{\mathrm{A,max}}^{\mathrm{s}} \frac{B_{\mathrm{s}}}{1 - p_{22}(1 - B_{\mathrm{s}})} \\ &E_{\mathrm{s}} = E_{\mathrm{A,max}}^{\mathrm{s}} \frac{p_{2\mathrm{s}}}{1 - p_{22}(1 - B_{\mathrm{s}})};\ E_{\mathrm{s,tot}} = E_{\mathrm{A,max}}^{\mathrm{s}} \frac{p_{2\mathrm{s}} B_{\mathrm{s}}}{1 - p_{22}(1 - B_{\mathrm{s}})} \end{aligned} \tag{6}$$

where $E_{\mathrm{A,tot}}^{\mathrm{op}}$, $E_{\mathrm{A,tot}}^{\mathrm{s}}$, and $E_{\mathrm{s,tot}}$ are the total energy influxes in all open antenna, "sink" antenna, and sink RCs, respectively.

As

$$F_{\mathrm{o}} = E_{\mathrm{A},0}^{\mathrm{op}} p_{2\mathrm{f}} \tag{7}$$

and, assuming that all centers are converted to sRCs

$$F_{\mathrm{m}}^{\mathrm{s}} = E_{\mathrm{A,max}}^{\mathrm{s}} (p_{2\mathrm{f}} + p_{2\mathrm{s}} p_{\mathrm{sf}}), \tag{8}$$

where $p_{2\mathrm{f}}$ and p_{sf} are the probabilities of fluorescence emission from the antenna and from sink centers, respectively and $F_{\mathrm{m}}^{\mathrm{s}}$ is the maximal fluorescence emission when all centers are sink centers.

Thus,

$$\begin{aligned} F_{\mathrm{op,t}} &= E_{\mathrm{A,tot}}^{\mathrm{op}} p_{2\mathrm{f}} = E_{\mathrm{A},0}^{\mathrm{op}} \frac{(1 - p_{22})(1 - B_{\mathrm{s}})}{1 - p_{22}(1 - B_{\mathrm{s}})} p_{2\mathrm{f}} \\ &= F_o \frac{(1 - p_{22})(1 - B_{\mathrm{s}})}{1 - p_{22}(1 - B_{\mathrm{s}})} \\ F_{\mathrm{s,t}} &= E_{\mathrm{A,tot}}^{\mathrm{s}} (p_{2\mathrm{f}} + p_{\mathrm{sf}}) \\ &= E_{\mathrm{A,max}}^{\mathrm{s}} \frac{B_{\mathrm{s}}}{1 - p_{22}(1 - B_{\mathrm{s}})} (p_{2\mathrm{f}} + p_{2\mathrm{s}} p_{\mathrm{sf}}) \\ &= F_{\mathrm{m}}^{\mathrm{s}} \frac{B_{\mathrm{s}}}{1 - p_{22}(1 - B_{\mathrm{s}})} \\ F_{\mathrm{t}} &= F_{\mathrm{op,t}} + F_{\mathrm{s,t}} = \frac{F_{\mathrm{o}}[(1 - p_{22})(1 - B_{\mathrm{s}})] + F_{\mathrm{m}}^{\mathrm{s}} B_{\mathrm{s}}}{1 - p_{22}(1 - B_{\mathrm{s}})}, \end{aligned} \tag{9}$$

which can be converted by substitution and simplification to:

$$\frac{F_{\mathrm{t}} - F_{\mathrm{o}}}{F_{\mathrm{m}}^{\mathrm{s}} - F_{\mathrm{o}}} = V_{\mathrm{t}} = \frac{B_{\mathrm{s}}}{1 - p_{22}(1 - B_{\mathrm{s}})} \tag{10}$$

This function yields a hyperbola with a horizontal asymptote and it can be applied to the experimental data (Fig. 2, yellow diamonds), albeit very roughly. Note that in this model $p_{2\mathrm{G}} = p_{22}$.

A better approximation is obtained if we consider that the conversion from closed to sRCs needs some kind of structural, conformational or biochemical change, which starts after the light is switched on and takes a time (τ) until it is completed (Fig. 1C). In this case, after a certain period there should be a variable population that would include opRCs, clRCs and sRCs. Both closed and sink centers are centers with Q_{A} reduced and then

$$B = B_{\mathrm{cl}} + B_{\mathrm{s}} \tag{11}$$

and

$$\frac{\mathrm{d}B_{\mathrm{s}}}{\mathrm{d}t} = kB_{\mathrm{cl}}, \tag{12}$$

where k is the rate constant for the conversion of B_{cl} to B_{s}. Therefore, after a time (t) the fraction of $B_{\mathrm{cl}} = Be^{-kt}$ (Eq. 12) and

$$B_{\mathrm{s}} = B(1 - e^{-kt}), \tag{13}$$

and then,

$$V_{cl} = \frac{B}{1 + Chyp(1 - B)} e^{-kt} \text{ (see Eq. 1)} \tag{14}$$

and

$$V_{\mathrm{s}} = \frac{B}{1 - p_{22}(1 - B)} (1 - e^{-kt}) \tag{15}$$

and consequently:

$$V = \frac{B}{1 + Chyp(1-B)} e^{-kt} + \frac{B}{1 - p_{22}(1-B)} (1 - e^{-kt}), \tag{16}$$

where

$$Chyp = \left(\frac{F_m}{F_o} - 1\right) p_{22}, \tag{17}$$

for this final model (Fig. 1C).

Results

Analysis of chlorophyll *a* fluorescence induction curves in the presence of DCMU

Chlorophyll *a* fluorescence transient usually shows three characteristic steps between minimal (O) and maximal (P) fluorescence emission intensity; these are K, J and I, which were clearly distinguished when plotted on a logarithmic time scale (Strasser and Govindjee 1991, 1992; Strasser et al. 2004; Lázár 1999). The K, J, I, and P steps corresponded, in the two Trebouxiophyceae genera studied here, to time intervals of about 0.3, 3, 60–80, and 300 ms, respectively (Fig. 3). The herbicide DCMU is an inhibitor of electron transport between the quinones Q_A and Q_B of PSII (Velthuys 1981; Stirbet and Govindjee 2011); it works by displacing Q_B from its binding site at the D1 protein of the PSII reaction center complex (Velthuys 1981). The fluorescence kinetics in the presence of DCMU represents the photosynthetic events leading to the complete closure of RCs (Lázár 1999; Strasser et al. 2004). Figure 3 shows the results obtained during the recording of fluorescence induction with a PEA fluorometer for samples maintained for 30 min in the dark and in the presence of 100 µM DCMU by careful addition of 500 µl of DCMU solution on to the algae disc in darkness. In contrast to control samples, Chl *a* fluorescence rise in DCMU-treated algae had a sigmoidal shape and did not show the K, J, I inflection points. DCMU-treated algae showed higher values of F_o than control samples. F_m values did not change, but the time needed to get F_m was shorter in DCMU-treated algae than in control ones (the rise time of DCMU-treated algae to F_m is similar to the rise time of the J level in uninhibited samples). Most of these results were similar to those extensively described for many species in previous works (Tóth et al. 2005; Stirbet and Govindjee 2012 and references therein). Tóth et al. (2005) reported for *Pisum sativum* leaves treated with DCMU that when the DCMU treatment was carried out in the presence of low light, the value of F_o significantly increased (at 1 µmol photons m^{-2} s^{-1} light intensity the F_o was ~48.5 % higher, and at

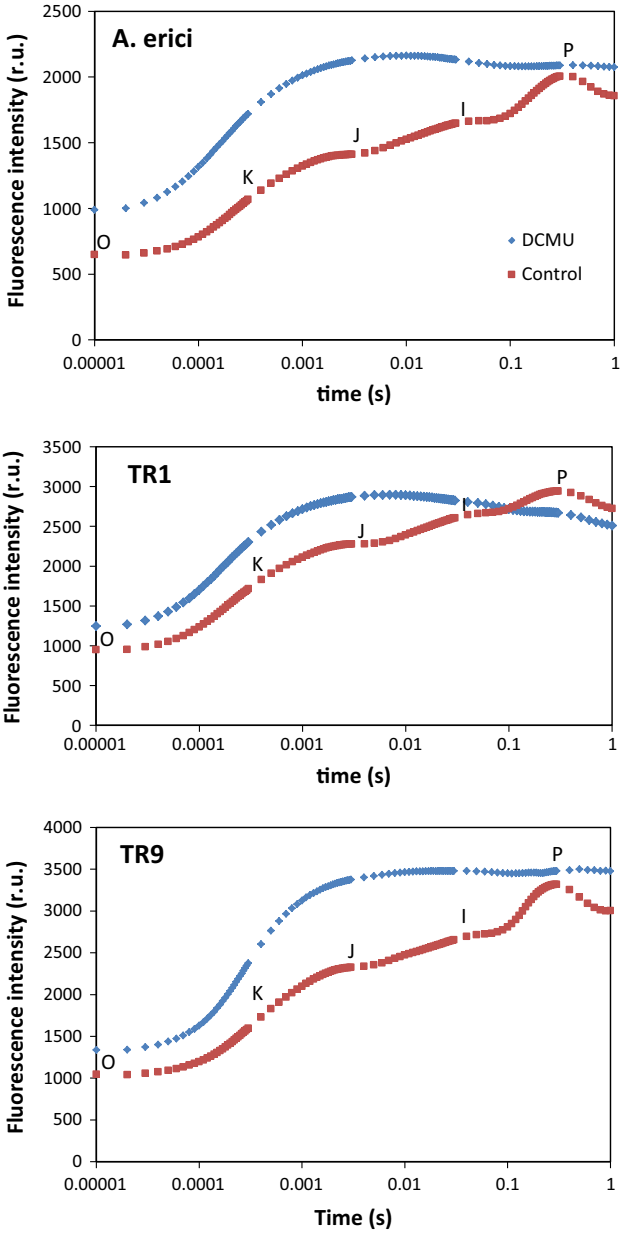

Fig. 3 Chlorophyll *a* fluorescence induction curves obtained in control (*red squares*) and DCMU-treated (*blue diamonds*) cultures of *Asterochloris erici*, and the *R. farinacea* phycobionts TR1 and TR9

0.3 µmol photons m^{-2} s^{-1}, it was ~39 % higher than the F_o of the non-DCMU-treated leaf discs). Therefore, it can be assumed that the small increase of F_o in DCMU-treated algae cells was a consequence of exposure to dim light (< 2 µmol photons m^{-2} s^{-1}) during the addition of DCMU or during the transport of the leaf discs from the petri dishes to the fluorometer.

To estimate the kinetics of Q_A reduction, the curve of fluorescence induction was normalized as V_t (Strasser et al. 2004), where $V_t = \frac{F_t - F_o}{F_m - F_o}$. Then, following Strasser et al. (2004),

$$B_t = \frac{\int_{o}^{t} (1 - V_t)\mathrm{d}t}{\int_{t_{fm}}^{} (1 - V_t)\mathrm{d}t} \equiv S_t,$$

where S_t represents the normalized complementary area at time t during the induction (the area between a line parallel to the t-axis joining F_m to the ordinates axis, and the induction curve represented as V_t) with respect to the total normalized complementary area (i.e. from $t = 0$ to $t = \max$), and B_t is the fraction of closed RCs (identical to the fraction of reduced Q_A) that has a value of zero when all the RCs are open, and 1 when all the RCs are closed. The model based on the energy flux theory (Strasser 1978, 1981; Strasser et al. 2004; Tsimilli-Michael and Strasser 2013) predicts that the B_t versus V_t curves approach a hyperbolic curve with a vertical asymptote (Fig. 1A). However, our experimental data for *A. erici* and for the TR1 (*Trebouxia jamesii*) and TR9 (*Trebouxia* sp.) phycobionts isolated from *R. farinacea* showed sigmoidal curves approaching a horizontal asymptote (Fig. 4A–C, blue circles). Therefore, an alternative model was needed to explain the behaviour of these microalgae.

We consider that some RCs could be converted from the closed state (closed RCs, clRCs) to a kind of energy sink (sink RCs, abbreviated as sRCs), where most of the energy input is converted into heat and fluorescence (Fig. 1B, C). This model is described by the following equation (see "Theory" section):

$$V = \frac{B}{1 + Chyp(1 - B)} e^{-kt} + \frac{B}{1 - p_{22}(1 - B)}(1 - e^{-kt}), \quad (16)$$

Figure 4A–C shows that this model is consistent with the experimental data for *A. erici* and *Trebouxia* TR1 and TR9 (blue circles). Multiparametric non-linear regression was performed using the programs Datafit 9® (Oakdale Engineering, Oakdale, PA, USA) and Sigma plot 10®. The computed R^2 values for the three studied phycobionts were higher than 0.999 (Table 1) and the model-predicted values (Fig. 4, red triangles) fitted well with the experimental values (Fig. 4, blue circles). The parameters calculated are shown in Table 1. The value of p_{22}, the probability of interconnection between RCs, was high in the three species, with maximal values for TR9 (~0.83) and minimal for TR1 (~0.65). On the other hand, TR1 had the highest value for the rate constant k for the conversion of closed into sink centers (~9500 s^{-1}) and TR9 the lowest (~3100 s^{-1}). These results show that a very active exchange of energy between PSII units is present in trebouxoid phycobionts. Equation 16, derived from this

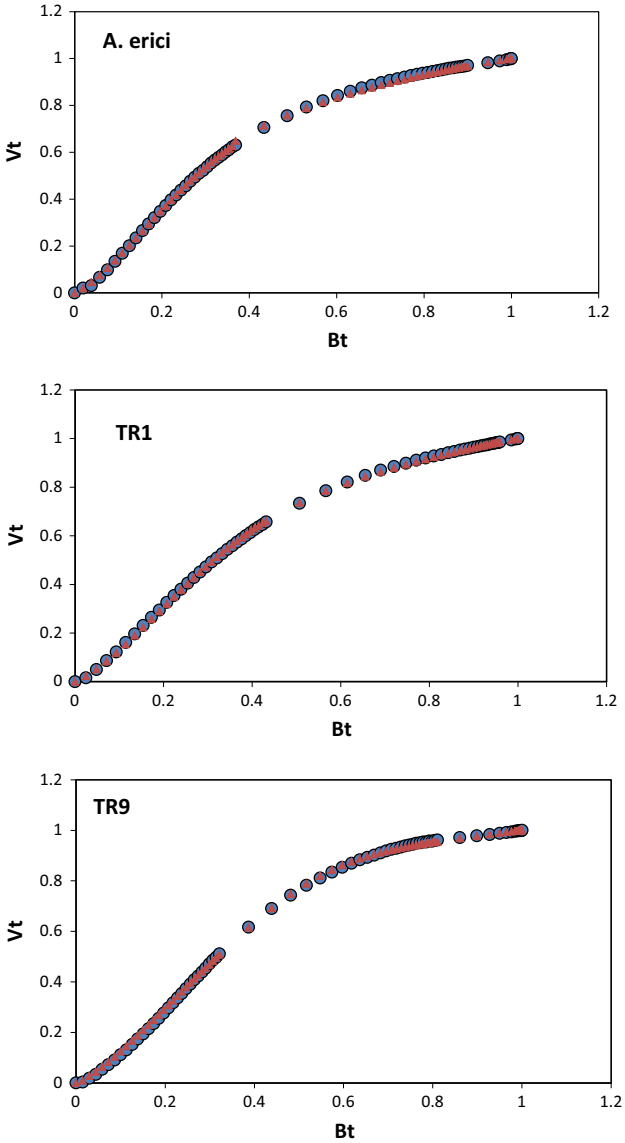

Fig. 4 Fitting of the model described by Eq. 16 to experimental data. *Blue circles* experimental data obtained for DCMU-treated cells; *red triangles* non-linear regression

Table 1 B_t (proportion of closed reaction centers) vs. V_t (variable fluorescence) curve parameters

Species	p_{2G}	K (s^{-1})	R^2
Asterochloris erici	0.7 ± 0.0	8912 ± 96	0.9996
TR1 (*Trebouxia jamesii*)	0.6476 ± 0.0029	9483 ± 157	0.9998
TR9 (*Trebouxia* sp.)	0.8266 ± 0.0461	3093 ± 8	0.9998

p_{2G} global probability for excitation energy transfer ("exciton" transfer) from one PSII unit to another, K rate constant for the transformation of closed centers to energy sink centers, R^2 regression coefficient

Results are the mean ± SE of 3–5 independent experiments

model, can be easily transformed to represent F_t as a function of time and it also fits very well to the original experimental data (Fig. 5A, C). Green triangles and purple circles, in Fig. 5A–C, represent the computed time-course for closed and sink units, respectively.

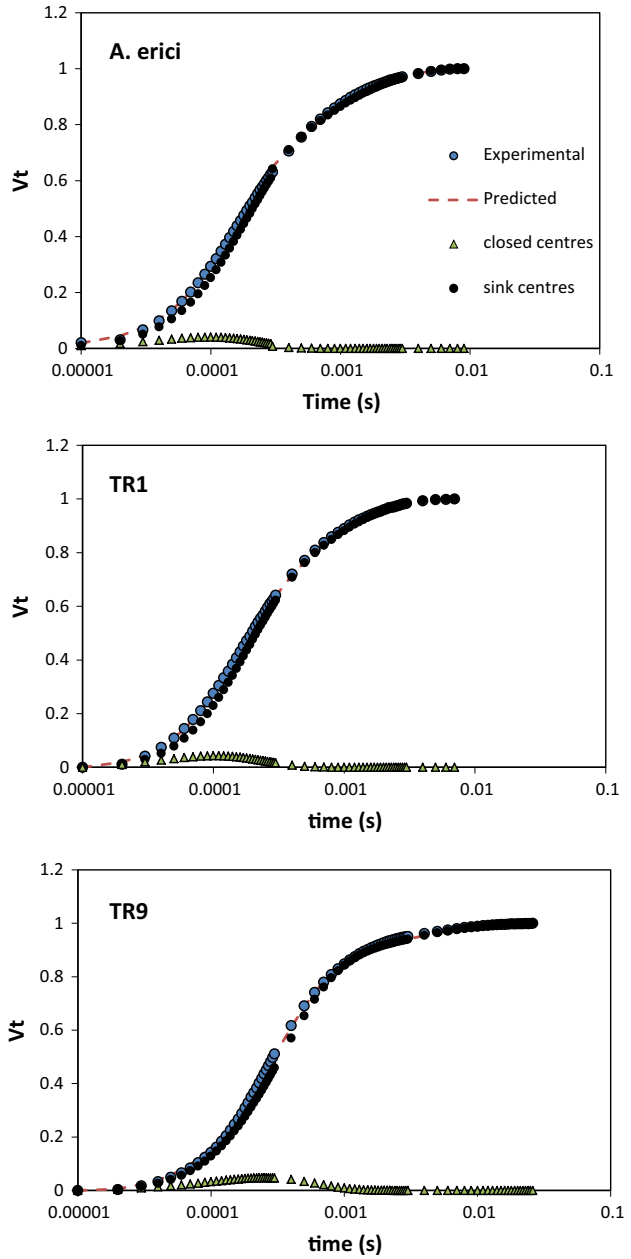

Fig. 5 Time course of relative variable fluorescence ($V_t = F_t - F_o / F_m - F_o$) in DCMU-treated cells. *Blue circles* experimental data obtained for DCMU-treated cells incubated for 30 min in the dark; *red discontinous line* non-linear regression results; *green triangles* calculated time course for closed RCs; *black circles* calculated time-course for sink centers. Results presented here are the mean from five different samples. There were no significant differences found when the experiments were repeated (five times, $n = 2$–5 per experiment) with different cultures (R^2 was always >0.99)

Figure 6 shows results obtained for TR9 when several saturating pulses (3000 µmol photons m^{-2} s^{-1}, 1 s) were applied, separated by dark time intervals of 1 s. In the presence of DCMU, there was a large increase in F_o between the first and second saturating pulses. The following pulses had only a small effect on the increase in F_o in DCMU-treated samples. The increase in F_o without a decrease in F_m in DCMU-treated samples indicated the presence of closed centers (centers with reduced Q_A) at the start of the second and successive saturating pulses. A quantification of closed centers at the start of the second and successive pulses is shown as an inset in Fig. 6. The proportion of closed RCs was calculated as:

$$1 - \frac{(F_v^*/F_m^*)}{(F_v/F_m)},$$

where F_v^* and F_m^* are respectively the variable Chl *a* fluorescence and the relative maximal fluorescence values for the second and successive pulses. Following the first pulse, around 39 % of the RCs were closed in DCMU-treated cells after 1 s of darkness; meanwhile there were only about 15 % clRCs in the untreated cells. The proportion of clRCs increased up to 46 % after another four successive saturation pulses in DCMU-treated cells, but remained constant in non-DCMU-treated cells. These results were

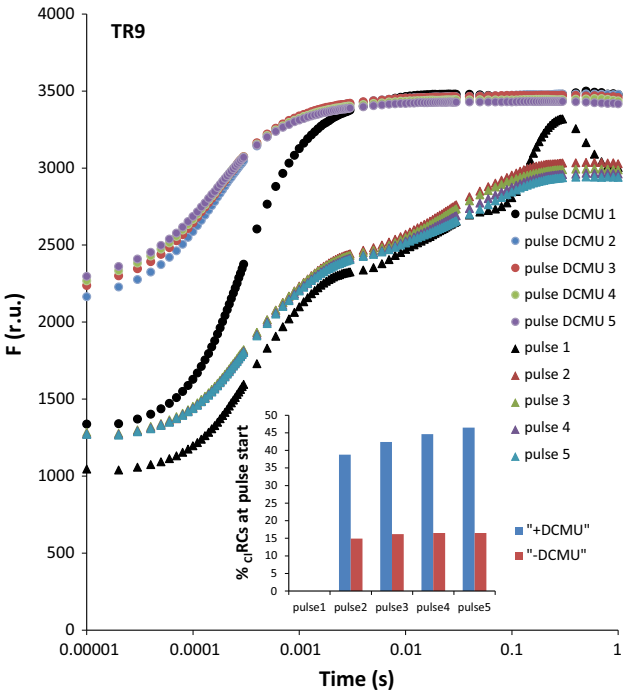

Fig. 6 Effect of successive high light pulses (3000 µmol photons m^{-2} s^{-1}) on the chlorophyll *a* fluorescence transient of TR9 control cells and those treated with DCMU. *Inset* fraction of closed reaction centers at the start of the second to the fifth saturation pulse in DCMU-treated (*blue bars*) and untreated (*red bars*) cells. See text for further details

expected because DCMU blocks electron transport beyond Q_A.

However, the reduction kinetics of the remaining open RCs during the successive light pulses in DCMU-treated cells can be adjusted to the model described by Eq. 16. Figure 7 shows that after the first pulse, the sigmoidicity of the B_t versus V_t curves was clearly diminished because there was a very fast rise of V_t at low B_t values in DCMU-treated cells. This is apparently a consequence of the increase in connectivity (Table 2, p_{2G}) and the increase in the value of the rate constant (Table 2, K) for the conversion of clRCs into sRCs. These results also showed that a large majority of RCs can be re-opened (Q_A oxidized) during the dark interval. The loss of sigmoidicity in the B_t versus V_t curves, and the apparent increase in the rate constant (K) could indicate that a proportion of the re-opened centers retained, at least partially, the characteristic of sRCs (the capacity to act as energy sinks). Figure 8 shows a spider-plot including some of the parameters of the so-called JIP-test (Strasser et al. 2000, 2004) calculated from fluorescence curves of DCMU-treated cells. The JIP-test is a frequently used tool for the rapid screening of many samples providing information about the structure, conformation and function of their photosynthetic apparatus (Strasser et al. 2000). The main disadvantage of this test is that the derived parameters (see below) are not direct measurements, but inferred quantities based on many assumptions (see Supplementary material). The use of spider-plots (also called "radar-plots") was recommended for the presentation of JIP-test results by Strasser et al. (2000) as a multi-parametric description of structure and function of each photosynthetic sample, presented by a polygonal line. According to Strasser et al. (2000), the spider-plot provides a direct visualization of the behaviour of a sample and thus facilitates the comparison of plant material. Strasser et al. (2004) defined the specific trapping flux (TR/RC) as the rate per RC, by which excitons are trapped by RCs resulting in the reduction of Q_A, i.e. in the increase in fraction B of closed RCs; hence TRt/RC (in arbitrary units), which is equal to dB_t/dt. TRo/RC expressing the specific trapping flux at time 0, can be calculated, according to Strasser's definition, by the extrapolation of dB/dt versus V_t curves to $V_t = 0$ (Supplementary material). We note than in the Strasser's original JIP-test, TRo/RC is calculated in a different way, taking as an assumption that the shape of the O–J part of a normal transient ($t < 2$ ms) measured in vivo is quite proportional to the O–J rise in the presence of DCMU (Strasser and Strasser 1995; Strasser and Stirbet 1998).

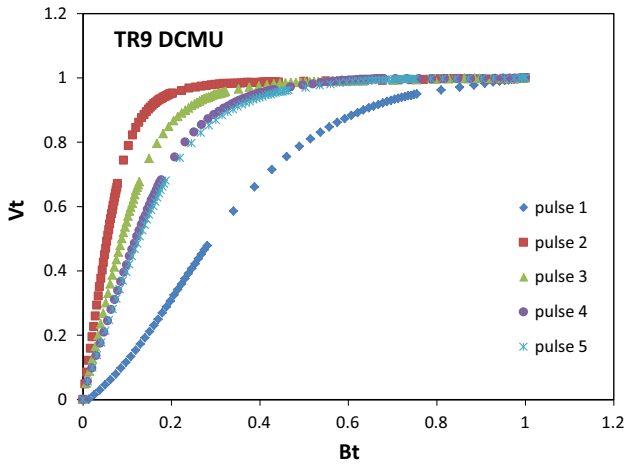

Fig. 7 B_t (proportion of closed RCs) vs. V_t (relative variable fluorescence) curves of TR9 DCMU-treated cells after successive light saturating pulses. For details of samples, and treatments, see Fig. 6 legend

Once the value of TRo/RC is obtained, it is easy to calculate other parameters of the JIP-test, as the absorption flux per active RC (ABS/RC = TRo/RC ($1/\varphi_{Po}$); $\varphi_{Po} = 1 - (F_o/F_m)$ = maximum quantum yield of primary photochemistry); the energy dissipation flux per active RC (Dio/RC = ABS/RC − TRo/RC) and the corresponding quantum yield of energy dissipation ($\varphi_{Do} = 1 - \varphi_{Po}$). In Fig. 8 we can see that the relative values of TRo/RC, ABS/RC, Dio/RC and φ_{Do} increased after every successive light pulse; meanwhile, the values of φ_{Po} (F_v/F_m), S_m (normalized

Table 2 B_t (proportion of closed reaction centers) vs. V_t (relative variable fluorescence) curve parameters in TR9 treated with 100 μM DCMU

Pulse	p_{2G}	K (s^{-1})	R^2	F_m	F_o	clRCs (%)
1	0.8212 ± 0.0023	3171 ± 4	0.9993	3504 ± 270	1335 ± 96	–
2	0.9845 ± 0.0006	5402 ± 99	0.9973	3484 ± 240	2164 ± 143	38.78
3	0.9764 ± 0.0010	5373 ± 106	0.9972	3475 ± 237	2237 ± 149	42.40
4	0.9636 ± 0.0020	5223 ± 140	0.9964	3453 ± 231	2267 ± 152	44.64
5	0.9562 ± 0.0023	5471 ± 159	0.9959	3436 ± 226	2297 ± 163	46.46

p_{2G} global probability for excitation energy transfer ("exciton" transfer) from one PSII unit to another, K rate constant for the transformation of closed centers to energy sink centers, R^2 regression coefficient, F_m maximal fluorescence, F_o minimal fluorescence, *clRCs* percentage of closed reaction centers at the start of the light pulse

Results are the mean ± SE of five independent experiments

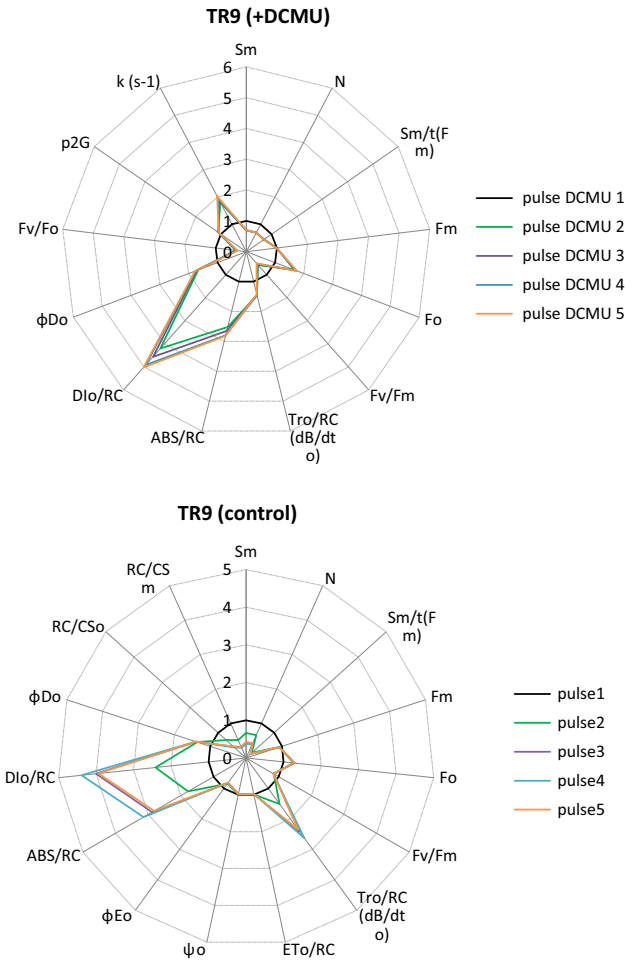

Fig. 8 Spider-plots (Strasser et al. 2000) showing the quantitative extent of changes in various fluorescence parameters during the application of successive saturating light pulses in DCMU-treated and untreated TR9 cells. Values are relatives to the first pulse for each treatment (*black circle* with radius 1). S_m complementary area normalized to variable fluorescence [Area/($F_m - F_o$)], N turnover number (expresses how many times Q_A has been reduced from time 0 to time F_m), S_m/t_{F_m} average excitation energy of open RCs; F_m, maximal fluorescence, F_o minimal fluorescence, F_v/F_m ratio of variable to maximal fluorescence, *TRo/RC* specific trapping flux at time 0, *ETo/RC* specific flux of electron transport at time 0, ψ_o probability that a trapped exciton moves an electron in the transport chain beyond Q_A, φ_{Eo} quantum yield of electron transport at time 0, φ_{Do} quantum yield of energy dissipated at time 0, *ABS/RC* absorption flux per RC, *DIo/RC* dissipated energy flux per RC at time zero, *RC/CSo* density of RCs (Q_A reducing PSII reaction centers) taking F_o as a measure of the cross section (CS) size, *RC/CSm* density of RCs (Q_A reducing PSII reaction centers) taking F_m as a measure of the cross section (CS) size, p_{2G} grouping probability, K rate constant for the transformation of closed centers to energy sink centers. Definitions of JIP-test parameters are from Strasser et al. (2000, 2004)

complementary area over the induction curve), N (turnover number) and S_m/t_{Fm} (average number of open centers in the time span from 0 to time F_m) (Appenroth et al. 2001), decreased. The increase in ABS/RC, indicated that the fraction ($\sim$60 %) of RCs reopened after the pulse during the dark interval received more energy. The increase in energy dissipated (DIo/RC, φ_D) was also coherent with the formation of sRCs and their function as energy dissipation traps.

Formation of sRCS in the absence of DCMU

The formation of sRCs in the presence of DCMU was probably induced by the blockage of electron transport beyond Q_A. We speculate that sRCs have a role in protection against excessive light under natural conditions. To test this hypothesis we have performed light treatments that can saturate the acceptor side of PSII. The first one was the application of several saturating pulses as described for DCMU-treated samples in the preceding section. This allows a direct comparison of results with and without DCMU treatment; but we need to take into account that in DCMU-untreated samples, the area complementary to the induction curves (S_m) diverges from B_t (fraction of closed RCs) because electron transport beyond Q_A is open, and also because fluorescence emission can be influenced by several factors, such as the redox state of the plastoquinone pool and the acceptor and donor sites of PSI (Tóth et al. 2007; Vredenberg and Bulychev 2003; Munekage et al. 2004; Stirbet and Govindjee 2012). In Fig. 6 we can see that after the first light pulse, samples that were not treated with DCMU had a much smaller increase in apparent F_o than DCMU-treated algae, but showed a decrease in F_m that was not observed in DCMU-treated samples. Subsequent pulses had no effect on F_o in control samples and only a small effect on F_m. The presence of three inflection points (K, J, I) in the induction curves of non-DCMU-treated samples was observable during the successive pulses, indicating that under these conditions there was not a massive blockage of electron transport. This was confirmed quantitatively by the analysis of the JIP-test, which did not show a decrease in the parameter Eto/RC (electron transport beyond Q_A *per* RC) during the successive light pulses (Fig. 8). Just as experiments in the presence of DCMU, untreated algae showed an increase in ABS/RC, TRo/RC, DIo/RC and φ_{Do} parameters after successive light pulses. As mentioned above, the complementary areas of the induction curves (S_m) in the absence of DCMU cannot be directly related to the state of Q_A reduction, as shown by the complex kinetics of the fluorescence transient of TR9 cells during a single saturation pulse of 3000 µmol photons m^{-2} s^{-1} (Fig. 9A, first pulse). However after this first pulse, the S_t versus V_t (complementary area vs. relative variable fluorescence yield) kinetics during the successive light pulses was simplified and approached hyperbolic curves with horizontal asymptotes (Fig. 9A, second and successive pulses). The second pulse data could be well fitted ($R^2 > 0.99$) to the double hyperbola equation

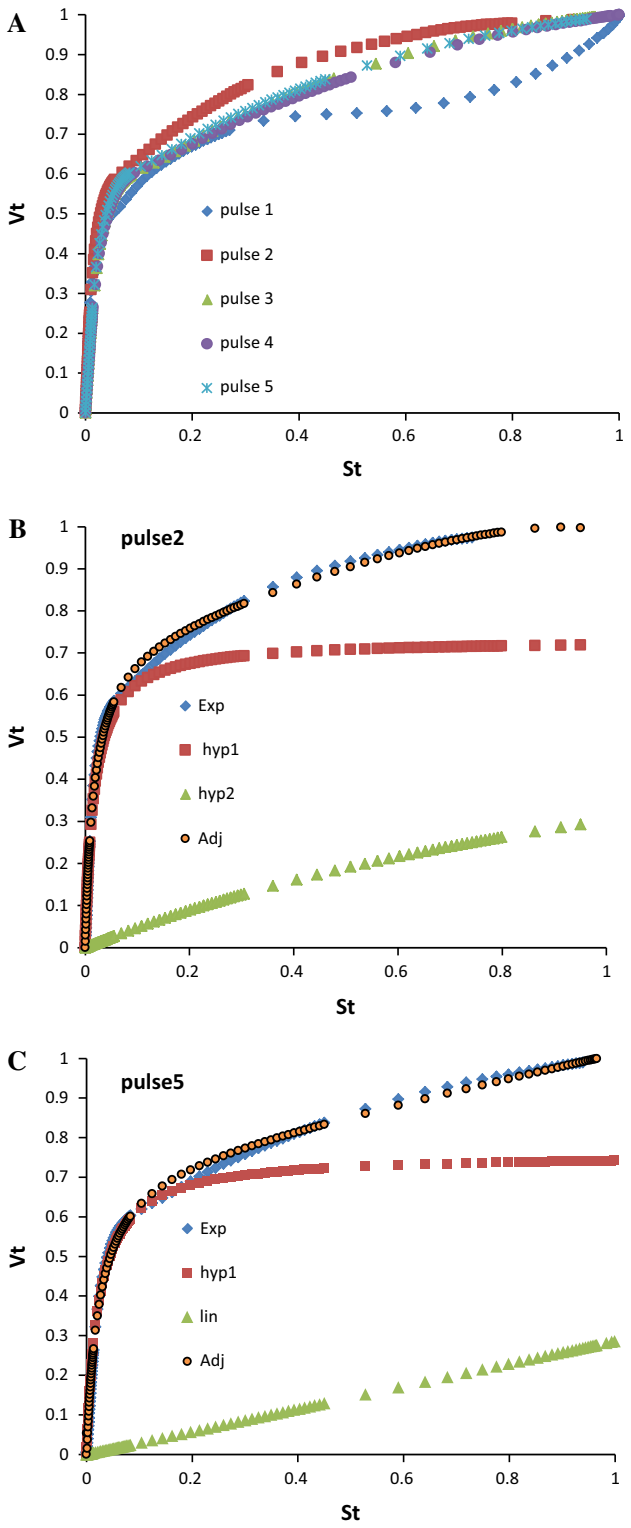

Fig. 9 **A** Complementary area (S_t) vs. variable fluorescence (V_t) curves for TR9 cells during successive saturating (1–5) pulses. **B** Fitting of the experimental data (*blue diamonds*) from the second pulse to Eq. 18 (*orange circles*) and deconvolution of the data in two hyperbolic curves (*red squares* and *green triangles*). **C** Like (**B**), but the data are from the fifth pulse and deconvolution is to a *hyperbolic curve* and a *straight line*. For further details, see text

$$V_t = a\frac{S}{1-p_{22}(1-S)} + b\frac{S}{1-p'_{22}(1-S)}, \tag{18}$$

where S is the complementary area and a, b represent the amplitudes (the respective asymptotes) for each hyperbola. This equation is derived from Eq. 10, but adapted to the hypothetic existence of two populations of RCs, each one characterized by a different connectivity (p_{22} and p'_{22}, respectively). We note that Eq. 10 describes the conversion of open centers into sink centers without mediation of conformational or structural changes. Figure 9B shows our experimental results (exp, blue diamonds) obtained during the application of a second saturating pulse, the results of fitting these data to Eq. 18 ($R^2 = 0.998$; orange circles) and the deconvolution of this curve into two horizontal hyperbola (hyp1, red squares; hyp2, red triangles). If every one of these hyperbola were related to a different population of active RCs, then the population described by hyp1 would contain about 72 % of the active RCs with very high connectivity ($p_{22} = 0.97$); and hyp2, 28 % of active RCs with low connectivity ($p'_{22} = 0.03$). During the third, fourth and fifth pulses the relative size (amplitude) of both populations was constant, but the population described by hyp2 lost the connectivity ($p'_{22} = 0$) and for this population, the evolution of V_t (variable fluorescence) as a function of St (complementary area) approached a straight line (Fig. 9C).

A second set of experiments was performed with a Dual-PAM 100 fluorometer. A standard recording of fluorescence induction and P700 oxidation kinetics was started with plants or algae that had been maintained for 20–30 min in the dark. A first saturating pulse was applied to determine the F_m and F_o values. After this first pulse, the sample was illuminated for 10 s with far red light (720 nm) and a second saturating pulse was applied to determine Pm (the maximal oxidation of P700). After a delay period in darkness, the actinic light was switched on and, after a short time, a third saturating pulse was applied. Then, successive pulses of saturating light were applied at fixed intervals. Figure 10A shows a typical Chl *a* fluorescence induction experiment carried out with *A. erici* cells. In this experiment pulses of saturating light (3000 µmol photons m^{-2} s^{-1}) were applied every 30 s in the presence of actinic light (120 µmol photons m^{-2} s^{-1}, λ_{max} 635 nm). The quantum yields of PSII (φ_{PSII}), as inferred from fluorescence data, and PSI (φ_{PSI}) fell to a minimum after switching on the actinic light, as is characteristic at the fluorescence emission maximum during the Kautsky transient for plant and algal material (Fig. 10A, third saturating pulse). Meanwhile, φ_{NPQ} (the yield of energy dissipated by downregulatory non-photochemical processes; Kramer et al. 2004) was still at very low values, but φ_{NO} (the yield of energy that is dissipated by other non-photochemical processes; Kramer et al. 2004) was high (corresponding to

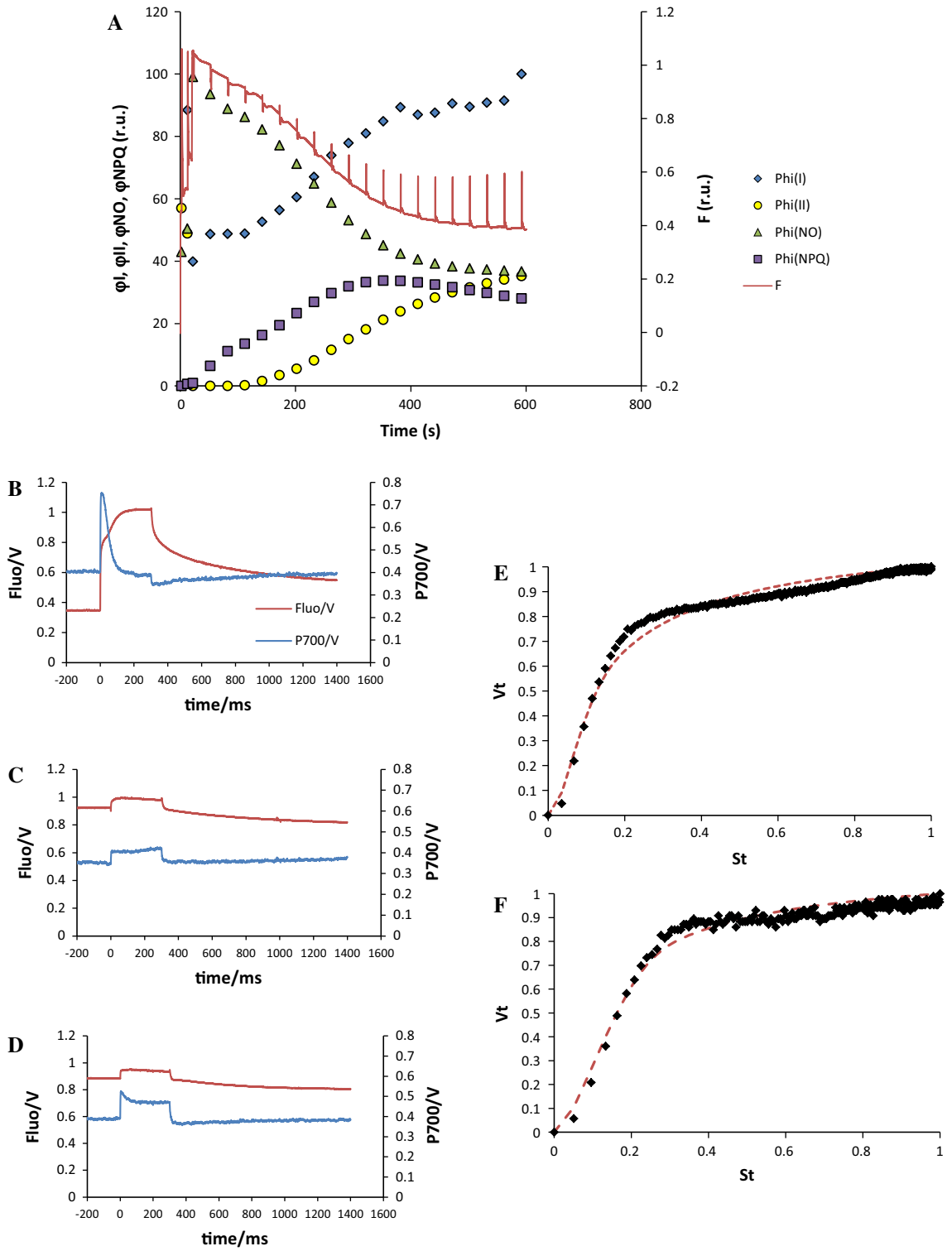

Fig. 10 **A** Fluorescence quenching analysis of *A. erici* cells by the saturation pulse method using modulated fluorescence with a Dual-PAM 100 fluorometer. *Red line* original recording of the fluorescence emission, *blue diamonds* quantum yield of PSI, *yellow circles* quantum yield of PSII (φ_{PSII}), *purple squares* yield for dissipation of light energy by downregulation (φ_{NPQ}), *green triangles* yield of energy dissipation by other non-photochemical losses including fluorescence (φ_{NO}). **B–D** Fluorescence (*red lines*) and P700 (*blue lines*) transients of the pulses 1, 2 and 3, respectively, of (**A**). **E** V_t vs. S_t curve of the third pulse of (**A**); *black triangles* experimental data, *red discontinuous lines* fitting to Eq. 16 ($R^2 = 0.96$, SE of estimate = 0.021). **F** As (**E**), but for the fourth pulse ($R^2 = 0.93$; SE of estimate = 0.035)

relative maxima of fluorescence emission). If we analyse the fluorescence transients obtained during the first pulses (Fig. 10B–D), we find in the first place that the basal fluorescence emission (apparent F_o) increased from the first to the fourth pulse, also that during the third and fourth pulses the characteristic OJIP shape of the fluorescence transient was lost (Fig. 10C, D) and finally that P700 was not reduced, indicating that electron transport beyond Q_A was blocked. In fact, during these pulses, the shape of the fluorescence induction curve was very similar to the transients observed after DCMU treatment. The *Bt* versus *Vt* curve approached a hyperbola with an horizontal asymptote Fig. 10E, F), as in the case of DCMU-treated cells that fits reasonable well ($R^2 > 0.96$) with Eq. 16, which describes the conversion of clRCs (closed reaction centers) to sRCs (sink reaction centers) accompanied by an structural or conformational change. Therefore, these results indicated that sRCs were transiently formed in algal cells in the absence of DCMU.

Discussion

The study of the kinetics of the fluorescence transient in the presence of DCMU has led to several authors to propose different models (for a comprehensive review see Stirbet and Govindjee 2012) to explain the relationship between the reduction of Q_A and the emission of fluorescence. It is well-established that the relationship between the propor-tion of reduced Q_A and fluorescence emission is non-linear, except in the case (puddle model) in which the RCs are not connected (Lavergne and Trissl 1995; Stirbet et al. 1998; Kramer et al. 2004; Strasser et al. 2004). Independent of the starting point of theoretical assumptions of different models, all of the models have used equations similar to Eq. 1 (see the "Theory" section), which establish a numerical relationship between the emission of fluores-cence and the reduction of Q_A in plants and algae. This equation describes a hyperbolic function with a vertical asymptote (Strasser et al. 2004) that has been demonstrated to be valid for most of the plants studied thus far, inde-pendent of the possible heterogeneity of their RCs, including the presence of non-Q_B reducing centers or of non-Q_A reducing silent centers (Strasser et al. 2000; Strasser et al. 2004; Schansker and Strasser 2005; Tsimilli-Michael and Strasser 2013). However, we show in this paper that the fluorescence kinetics of *A. erici* and the *Trebouxia* TR1 and TR9 phycobionts of *R. farinacea* cannot be fitted to this function, as its relation with variable fluorescence approaches a horizontal asymptote (Fig. 8C). This type of curve has been obtained in studies on higher plants exposed to very low temperatures (77°K) (Strasser and Greppin 1981). Those results were explained in a model that considers the following points: 1) at low temperatures an acceptor pool surrounds the RC complex so that a closed RC can become open again; 2) the primary acceptor pool Q can transfer electrons to several neighbour units; and 3) at room temperature, and in the presence of DCMU, a secondary acceptor R (plastoquinone) is reduced, preventing the reopening of the closed reaction center. However, the equations derived to describe this model do not fit in with our experimental results with *A. erici* and the phycobionts TR1 (*Trebouxia jamesii*) and TR9 (*Trebouxia* sp.) ($R^2 < 0.90$).

We have considered here several approaches based on Strasser's theory of energy fluxes (Strasser 1978, 1981, 1986; Stirbet et al. 1998, 2004; Strasser and Tsimilli-Michael 2001; Tsimilli-Michael and Strasser 2013). The best fit to the experimental results for DCMU-treated algae was obtained by using Eqs. 2–16 (Fig. 4). These equations describe a model (Fig. 1D) that assumes the following: (1) after closure of RCs, they are converted into sink centers (sRCs); (2) the probability of energy leaving the sRCs is very low or zero, thus sRCs centers act as true energy traps; (3) sRCs have the same fluorescence yield as closed centers (F_m is not changed by DCMU treatments); (4) the connectivity of PSII units with sRCs (sPSII) with other PSII units is only one-way, i.e. energy can be transferred from other PSII units to sPSII units, but not from sPSII units to other PSII units; and (5) the conversion from closed RCs to sRCs requires a structural, biochemical or conformational change. This model fits perfectly ($R^2 > 0.99$) with the original (F_t vs. time) experimental data (Fig. 4).

Cleland et al. (1985) proposed that a direct effect of photoinhibition is a permanent modification of PSII reaction centers that makes them incapable of generating charge separation (inactive RCs) but highly efficient in trapping and in the dissipation of light energy. Krause et al. (1990), in a study with isolated thylakoids, proposed that photoinhibition is based on transformation of active RCs to photochemically inactive fluorescence quenchers, which convert excitation energy to heat. The existence of these "heat sinks" (Krause 1988), or "silent reaction centers" (Strasser et al. 2004) was also supported by results employing the so-called JIP-test analysis (Krüger et al. 1997; Strasser and Tsimili-Michael 1998), which showed that in organisms exposed to light or heat stress, a pronounced decrease in F_v/F_m and in stability of TRo/RC (trapped electrons per RC at $t = 0$) occurs, while no absorption changes were detected. Strasser and Tsimili-Michael (1998) proposed that this apparent controversy is due to the transformation of some RCs that, after a conformational change, act as efficient exciton traps but dissipate all their excitation energy as heat from both the antenna and the modified RC (see Strasser et al. 2004; Tsimilli-Michael and Strasser 2013 for a model). The

formation of silent centers has been proposed to perform a protective role against certain stresses (Thach et al. 2007; Bussotti et al. 2011; Mathur et al. 2011) or a response to the application of some growth inhibitors (Sánchez-Muñoz et al. 2012). According to Tsimilli-Michael and Strasser (2013), the conformation of an inactive center compared to that of open RC is characterised by the substitution of the rate constant (k_{bP}) of the reaction PA → $P^+ A^-$ (P standing for P680, i.e. the PSII RC, and A for the primary electron acceptor of PSII) by a dissipation rate constant k_{bQ} of equal magnitude. Concomitantly, the silent centers, throughout the fluorescence induction, behave in respect to their fluorescence yield as open RCs but cannot become closed (Tsimilli-Michael and Strasser 2013). However, as far as we know, no structural model has been proposed for silent reaction centers.

The sRCs, described in this paper, share some common characteristics with silent centers, such as the capacity for exciton trapping and the dissipation of this energy to avoid damage to the photosynthetic machinery. However, there are many differences between "traditional" silent centers and sRCs. Firstly, sRCS are not a permanent form of inactive centers, because they can be reoxidized (during a short period in darkness) and re-reduced as evidenced by experiments applying several successive saturating light pulses to DCMU-treated algae (Figs. 6, 7). The main pathway of Q_A^- re-oxidation in the presence of DCMU is the recombination of the electron on Q_A^- with the positive charge located in the water oxidizing complex (in the S_2 state if the illumination was given to a dark-adapted sample). The half-time of this process, as measured from the decay of the high fluorescence yield in the dark after a single turnover flash or from thermoluminescence emission is ca. 1 s (Robinson and Crofts 1983, Keren et al. 1997). The partial increase in the F_o level after the illumination, i.e. a residual fraction of centers in which Q_A^- cannot be re-oxidized, can be explained by the formation of non-recombining states, such as $S_1Tyr_D + Q_A^-$ in centers, which had reduced Tyr_D before the flash, i.e. $S_1Tyr_DQ_A$ → S_2-$Tyr_DQ_A^-$ → $S_1Tyr_D + Q_A^-$. The much smaller increase after the second and following flashes is due to the almost complete oxidation of Tyr_D by the first flash (Lavergne and Leci 1993; Keren et al. 1997; Vredenberg et al. 2006; Msilini et al. 2011).

The application of successive saturating pulses, in DCMU-treated algae (Fig. 8), results in an increase of connectivity (p_{2G}), an increase of the rate constant K and an increase of several parameters of the JIP-test, such as ABS/RC (energy absorbed per RC), TRo/RC (trapped energy per RC) and DIo/RC (energy dissipated per RC). The increase in ABS/RC has been associated with the formation of silent centers, but the accumulation of this kind of centers is also associated to a decrease in F_m (not observed in DCMU-treated Trebouxiophyceae algae) and the increase in ABS/RC is not accompanied by an increase in TRo/RC. On the other hand, the increase in ABS/RC indicates, generally speaking, an apparent increase in the size of the antenna. This "apparent" increase does not mean, in many cases, a "real" increase in the physical antenna complex size; for instance, there is no increase in the physical antenna size for the case of the "silent centers" mentioned above. In the case of DCMU-treated Trebouxiophyceae algae, the increase in the energy absorbed per RC (ABS/RC) can be due to several factors, such as the increase in connectivity (p_{2G}), or the establishment of an effective transfer of energy from the closed centers (that increase F_o, but do not contribute to variable fluorescence) to the open (active) RCs. The latter implies that those RCs that remained closed (40–50 %) after a period in darkness between the successive pulses do not behave as energy sinks. Joliot and Joliot (1964, 2003) described a p (connectivity) value ca. 0.7. The values presented in Table 1 of our paper are in the range 0.65–0.82. The connectivity parameter reaches higher values when successive saturating pulses in the presence of DCMU are applied (Table 2). As discussed by Slavov et al. (2013), the thylakoids of green microalgae do not have a differentiation between grana stacks and stroma membranes and this fact can facilitate rearrangements of the photosynthetic complexes. Slavov et al. (2013) propose that a drying-induced reorganization of the thylakoid membrane, which changes the relative association and distance of PSII and PSI particles, allows an energy "spillover" from PSII to PSI. Changes in the ultrastructure of the thylakoid membranes during desiccation of *A. erici* can be observed by transmission electron microscopy (Gasulla et al. 2013). According to our data, blockage of electron transport in the hydrated state under high illumination increases connectivity among PSII units. We can hypothesize that the architecture of green microalgae thylakoid membranes also facilitates rearrangements of the photosynthetic complexes in the hydrated state, allowing a grouping of PSII units under photooxidative stress conditions. This grouping facilitates a redistribution of the excess of energy and its redirection to sRCs. Finally, if at the start point of the second and subsequent pulses of a succession of light pulses, some of the open centers behave as sRCs unidirectionally capturing energy from closed RCS, a large increase of the ABS/RC would be expected, as well as an increase in the apparent value of the rate constant K and TRo/RC (trapped energy per RC at time zero). This explanation is consistent with the data presented in Fig. 8.

The horizontal hyperbola shape of the B_t versus V_t (fraction of closed RCs vs. variable fluorescence) curves found in the three microalgae that belong to the family Trebouxiophyceae studied here, can be readily interpreted

as a rapid increase in energy dissipation (rapid increase of fluorescence emission), which competes with energy redistribution from the closed centers. This behaviour, according to our model (Eq. 17; Fig. 1C), would be the consequence of the formation of sink RCs (sRCs). In the same way, the increase in DIo/RC (energy dissipated by RC at time zero) and φ_{Do} (yield of energy dissipated) for successive light pulses on the DCMU-treated algal cells (Fig. 8) indicates an increase in energy dissipation by sRCS. Therefore, the JIP-test data of DCMU-treated *Trebouxia* cells are consistent with the model proposed for sRCs.

We also investigated if the formation of sink RCs was possible in the absence of DCMU. We observed that in experiments where successive saturating pulses were applied (Fig. 9), after the second pulse, the S_m (complementary area) versus V_t (relative variable fluorescence) curves approach a horizontal hyperbola. This curve can, in turn, be deconvoluted (Eq. 18) to two horizontal hyperbolic functions, each one representing a sub-population of active RCs with different connectivity (p_{2G}). The main subpopulation ($\sim$72 % of the active RCs) remains constant in size and with a very high connectivity (p_{2G} $\sim$0.97) from the second until the last (fifth) pulse (Fig. 9B, C, red squares). However the second subpopulation (Fig. 9B, C, green triangles) was characterized by low connectivity after the first pulse (p_{2G} $\sim$0.03) which is lost ($p_{2G} = 0$) after the following pulses. We emphasize here that the only solution that we have found (following Strasser's energy flux theory for a bipartite model) to explain the occurrence of horizontal hyperbola in B_t (proportion of closed RCs) versus V_t (relative variable fluorescence) curves is the formation of RCs that apparently behave as energy sinks which take excitation unidirectionally from other RCs (Fig. 1B). Hence, the formation of sRCs is not restricted to DCMU-treated algae. Further, we found that when performing the saturation-pulse kinetic method, at the fluorescence emission maximum during the Kautsky transient, when φ_{PSII} is at a minimum and φ_{NO} (the proportion of energy trapped by PSII that is neither transformed in photochemistry nor in NPQ) is at a maximum, the St (complementary area) versus V_t curves derived from the fluorescence transient are also hyperbola with a horizontal asymptote, which fit in with Eq. 16. Then, the questions arise about how light energy captured by all the centers can be unidirectionally directed to sRCs and what is the nature of these centers. We suggest, as a hypothetical explanation, that the excitation energy, after the RCs are closed, can be directed to alternative acceptors which act as actual energy sinks. In other words, after closure of the RCs, an energy spillway is opened and this energy is directed to a sink. Consequently, it implies that the probability of energy transfer from the antenna to that sink (in a sRC) becomes greater than the probability of returning energy to another antenna system. This hypothesis can be supported by earlier observations, most of them related to desiccation-associated processes in poikilohydric photoautotrophs (Kopecky et al. 2005; Kranner et al. 2005; Heber and Shuvalov 2005; Heber et al. 2006). There is, for instance, increasing evidence for zeaxanthin-independent dissipation of excess light energy within the RC of PSII, involving several possible pathways for non-radiative Q_A^- decay (Ivanov et al. 2008; Yamakawa et al. 2012). Heber et al. (2007) proposed that desiccation-induced conformational changes of a chlorophyll protein complex result in fast, radiation-less dissipation of absorbed light energy. In another article, Heber et al. (2011) concluded that: "under desiccation, photoprotection is achieved by drainage of light energy to dissipating centers outside the RCs before stable charge separation can take place". Reversible quenching of fluorescence by strong illumination is suggested to indicate the conversion of the RCs from energy conserving to energy dissipating units. This permits them to avoid photoinactivation". Slavov et al. (2013) described that in the hydrated state of *Parmelia* lichen, a special far red (F740) emitting antenna complex is present. This complex would become a quencher in the desiccated state, although no pronounced quenching is observed in the hydrated state. Slavov et al. (2013) proposed that PSII in the hydrated lichen is in a kind of "semi-quenched" state where a small amount of Chl $-$ Chl charge transfer states are formed in the antenna, which, however, does not lead to a pronounced quenching yield. Treves et al. (2013) made a first report of a desert *Chlorella* (in the same group—Trebouxiophyceae—of green microalgae as the study species) with a very large, regulatable capacity to dissipate excitation, possibly through accelerated re-combinations. Since the desert *Chlorella* faces challenges similar to the lichen Trebouxiophyceae phycobionts studied here, we could be uncovering a related phenomenon, which may prove to be a property of this group of green microalgae. Interestingly, Heber (2008) found that better protection is achieved during the dry state if the chlorolichen was desiccated under light rather than under darkness. Activation of zeaxanthin-dependent energy dissipation by protonation of the PsbS protein of thylakoid membranes was not responsible for the increased loss of chlorophyll fluorescence by the lichen *Cladonia rangiformis* during drying in light. Heber (2008) concludes that light interacts with structural changes providing increased photoprotection.

The ecophysiological significance of the formation of sink centers could be to prevent damage under strong fluctuating light conditions when lichens are in a hydrated state, such as at the end of diurnal spring or summer storms. Frequent drying and wetting cycles, and the correlated inactivation and re-activation of photosynthesis,

leads to a pattern observed in most terrestrial habitats and produced, for example, by nocturnal dewfall or fog (Lange 1970; Kershaw 1985; Pospisil and Dau 2000; Okegawa et al. 2010). Sunrise activates net photosynthesis (CO_2 exchange above the zero line), but the peak is not reached until 1–2 h later, when the water content of the lichen starts to decrease (Lange 1970; Kershaw 1985; Belnap et al. 2003; Lange et al. 2006; del Prado and Sancho 2007). The net photosynthesis rate of lichens depends in a large part on the water content of their thalli (Lange et al. 2006; del Prado and Sancho 2007; Belnap et al. 2003). In many lichens, when the thallus is fully saturated with water, diffusion of CO_2 to the chlorobiont is hindered, and the CO_2 assimilation rate does not reach a maximum (Lange and Tenhunen 1981), thus potentially exposing the organism to light damage. This scenario can be avoided by invoking the mechanism discussed in this paper, as it will contribute to preventing light damage during excess of light or after an abrupt change of light intensity when the lichen is fully hydrated.

Acknowledgments This study was funded by the Spanish Ministry of Science and Innovation (CGL2009-13429-C02-00), Ministerio de Economía y Competitividad (MINECO CGL2012-40058-C02-01/02), FEDER, the Generalitat Valenciana (PROMETEO 2 2013/021 GVA) and the University of Alcalá/CAM (UAH2011/BIO 001). Mr. Daniel Sheerin has reviwed the English version of this paper. We thank all the 3 reviewers of this paper for their valuable comments since they helped us greatly improve our paper.

References

Ahdmajian V (1973) Methods of isolating and culturing lichen symbionts and thalli. In: Ahmadjian V, Hale ME (eds) The lichens. Academic Press, New York, pp 653–659

Allen JF, Mullineaux CW, Sanders CE, Melis A (1989) State transitions, photosystem stoichiometry adjustment and non-photochemical quenching in cyanobacterial cells acclimated to light absorbed by photosystem I or photosystem II. Photosynth Res 22:157–166

Appenroth KJ, Stöckel J, Srivastava A, Strasser RJ (2001) Multiple effects of chromate on the photosynthetic apparatus of *Spirodela polyrhiza* as probed by OJIP chlorophyll *a* fluorescence measurements. Environ Pollut 115:49–64

Baker NR (2008) Chlorophyll fluorescence: a probe of photosynthesis in vivo. Annu Rev Plant Biol 59:89–113

Barták M, Gloser J, Hájek J (2005) Visualized photosynthetic characteristics of the lichen Xanthoria elegans related to daily courses of light, temperature and hydration: a field study from Galindez Island, maritime Antarctica. Lichenologist 37:433–443

Belnap J, Büdel B, Lange OL (2003) Structure and functioning of biological soil crusts: a synthesis. In: Belnap J, Lange OL (eds) Biological soil crust: structure, function and management. Springer, Berlin, pp 3–30

Bilger W, Rimke S, Schreiber U, Lange OL (1989) Inhibition of energy-transfer to photosystem II in lichens by dehydration: different properties of reversibility with green and blue-green phycobionts. J Plant Phys 134:261–268

Bold HC, Parker BC (1962) Some supplementary attributes in the classification of *Chlorococcum* species. Arch Mikrobiol 42:267–288

Bukhow NG, Carpentier R (2004) Effects of water stress on the photosynthetic efficiency of plants. In: Papageorgiou GC, Govindjee G (eds) Chlorophyll *a* fluorescence: a signature of photosynthesis. Springer, Dordrecht, pp 623–635

Bussotti F, Desotgiua R, Cascioa C, Pollastrini M, Gravanoa E, Gerosab G, Marzuoli R, Nali C, Lorenzini G, Salvatori E, Manesd F, Schaube M, Strasser RJ (2011) Ozone stress in woody plants assessed with chlorophyll *a* fluorescence. A critical reassessment of existing data. Environ Exp Bot 73:19–30

Casano LM, del Campo EM, García-Breijo FJ, Reig-Armiñana J, Gasulla F, del Hoyo A, Guéra A, Barreno E (2011) Two Trebouxia algae with different physiological performances are ever-present in lichen thalli of *Ramalina farinacea*. Coexistence versus competition? Environ Microbiol 13:806–818

Cleland RE, Melis A, Neale PJ (1985) Mechanism of photoinhibition: photochemical reaction center inactivation in system II of chloroplasts. In: Amesz J, Hoff AJ, Van Gorkum HJ (eds) Current topics in photosynthesis. Martinus Nijhoff Publishers, Dordrecht, pp 77–86

del Prado R, Sancho LG (2007) Dew as a key factor for the distribution pattern of the lichen species *Teloschistes lacunosus* in the Tabernas Desert (Spain). Flora 202:417–428

Duysens LMN, Sweers HE (1963) Mechanism of two photochemical reactions in algae as studied by means of fluorescence. In: Japan Society of Plant Physiologists (eds) Studies on microalgae and photosynthetic bacteria. University of Tokyo Press, Tokyo, pp 353–372

Fernández-Marín B, Becerril JM, García-Plazaola JI (2010) Unravelling the roles of desiccation-induced xanthophyll cycle activity in darkness: a case study in *Lobaria pulmonaria*. Planta 231(6):1335–1342

Fos S, Deltoro VI, Calatayud A, Barreno E (1999) Changes in water economy in relation to anatomical and morphological characteristics during thallus development in *Parmelia acetabulum*. Lichenologist 31:375–387

Gasulla F, de Nova PG, Esteban-Carrasco A, Zapata JM, Barreno E, Guéra A (2009) Dehydration rate and time of desiccation affect recovery of the lichenic algae *Trebouxia erici*: alternative and classical protective mechanisms. Planta 231:195–208

Gasulla F, Guéra A, Barreno E (2010) A simple and rapid method for isolating lichen photobionts. Symbiosis 51:175–179

Gasulla F, Jain R, Barreno E, Guéra A, Balbuena TS, Thelen JJ, Oliver MJ (2013) The response of *Asterochloris erici* (Ahmadjian) Skaloud et Peksa to desiccation: a proteomic approach. Plant Cell Environ 36:1363–1378

Goldsmith SJ, Thomas MA, Gries C (1997) A new technique for photobiont culturing and manipulation. Lichenologist 29:559–569

Govindjee (1995) Sixty-three years since Kautsky: chlorophyll *a* fluorescence. Aust J Plant Physiol (now Funct Plant Biol) 22:131–160

Govindjee (2004) Chlorophyll *a* fluorescence: a bit of basics and history. In: Papageorgiou GC, Govindjee G (eds) Chlorophyll *a* fluorescence: a signature of photosynthesis. Advances in photosynthesis and respiration. vol 19. Springer, Dordrecht, pp 1–42

Govindjee Amesz J, Fork DC (eds) (1986) Light emission by plants and bacteria. Academic Press, Orlando (now available from Elsevier)

Green TGA, Nash TH III, Lange OL (2008) Physiological ecology of carbon dioxide exchange. In: Nash TH III (ed) Lichen biology. Cambridge University Press, Cambridge, pp 152–181

Heber U (2008) Photoprotection of green plants: a mechanism of ultra-fast thermal energy dissipation in desiccated lichens. Planta 228:641–650

Heber U, Shuvalov VA (2005) Photochemical reactions of chlorophyll in dehydrated Photosystem II: two chlorophyll forms (680 and 700 nm). Photosynth Res 84:85–91

Heber U, Lange OL, Shuvalov VA (2006) Conservation and dissipation of light energy as complementary processes: homoiohydric and poikilohydric autotrophs. J Exp Bot 57:1211–1223

Heber U, Azarkovich M, Shuvalov V (2007) Activation of mechanisms of photoprotection by desiccation and by light: poikilohydric photoautotrophs. J Exp Bot 58:2745–2759

Heber U, Soni V, Strasser RJ (2011) Photoprotection of reaction centers: thermal dissipation of absorbed light energy vs charge separation in lichens. Phys Plantarum 142:65–78

Ivanov AG, Sane PV, Hurry V, Oquist G, Huner NPA (2008) Photosystem II reaction centre quenching: mechanisms and physiological role. Photosynth Res 98:565–574

Jensen M, Chakir S, Feige GB (1999) Osmotic and atmospheric dehydration effects in the lichens *Hypogymnia physodes*, *Lobaria pulmonaria*, and *Peltigera aphthosa*: an in vivo study of the chlorophyll fluorescence induction. Photosynthetica 37:393–404

Joliot P, Joliot A (1964) Etudes cinétiques de la réaction photochimique libérant l'oxygene au cours de la photosynthese. C R Acad Sci 258:4622–4625

Joliot P, Joliot A (2003) Excitation energy transfer between photosynthetic units: the 1964 experiment. Photosynth Res 76:241–248

Keren N, Berg A, Paul JM, Van Kan PJ, Levanon H, Ohad I (1997) Mechanism of photosystem II photoinactivation and D1 protein degradation at low light: the role of back electron flow. Proc Natl Acad Sci USA 94:1579–1584

Kershaw KA (1985) Physiological ecology of lichens. Cambridge University Press, New York

Komura M, Yamagishi A, Shibata Y, Iwasaki I, Shigeru Itoh (2010) Mechanism of strong quenching of photosystem II chlorophyll fluorescence under drought stress in a lichen, *Physciella melanchla*, studied by subpicosecond fluorescence spectroscopy. Biophys Biochim Acta 1797:331–338

Kopecky J, Azarkovich M, Pfundel EE, Shuvalov VA, Heber U (2005) Thermal dissipation of light energy is regulated differently and by different mechanisms in lichens and higher plants. Plant Biol 7:156–167

Kramer DM, Johnson G, Kiirats O, Edwards GE (2004) New fluorescence parameters for the determination of Q_A redox state and excitation energy fluxes. Photosynth Res 79:209–218

Kranner I, Zorn M, Turk B, Wornik S, Beckett RR, Batic F (2003) Biochemical traits of lichens differing in relative desiccation tolerance. New Phytol 160:167–176

Kranner I, Cram WJ, Zorn M, Wornik S, Yoshimura I, Stabentheiner E, Pfeifhofer HW (2005) Antioxidants and photoprotection in a lichen as compared with its isolated symbiotic partners. Proc Natl Acad Sci USA 102:3141–3146

Krause GH (1988) Photoinhibition of photosynthesis. An evaluation of damaging and protective mechanisms. Physiol Plantarum 74:566–574

Krause GH, Weis E (1991) Chlorophyll fluorescence and photosynthesis—the basics. Annu Rev Plant Phys 42:313–349

Krause GH, Somersalo S, Zumbusch E, Weyers B, Laasch H (1990) On the mechanism of photoinhibition in chloroplasts. Relationship between changes in fluorescence and activity of photosystem II. J Plant Physiol 136:472–479

Krüger GHJ, Tsimilli-Michael M, Strasser RJ (1997) Light stress provokes plastic and elastic modification in structure and function of Photosystem II in camellia leaves. Physiol Plantarum 101:265–287

Lange OL (1970) Experimentell-ökologische Untersuchungen and Flechten der Negev-Wüste. I. CO_2-Gaswechsel von *Ramalina maciformis* (Del.) Bory unter kontrollierten Bedingungen im Laboratorium. Flora B 158:324–359

Lange OL, Tenhunen JD (1981) Moisture content and CO_2 exchange of lichens. II. Depression of net photosynthesis in Ramalina maciformisat high water content is caused by increased thallus carbon dioxide diffusion resistance. Oecologia 51:426–429

Lange OL, Green TGA, Melzer B, Meyer A, Zellner H (2006) Water relations and CO_2 exchange of the terrestrial lichen *Teloschistes capensis* in the Namib fog desert: measurements during two seasons in the field and under controlled conditions. Flora 201:268–280

Lavergne J, Leci E (1993) Properties of inactive photosystem II centers. Photosynth Res 35:323–343

Lavergne J, Trissl HW (1995) Theory of fluorescence induction in Photosystem-II—derivation of analytical expressions in a model including exciton-radical-pair equilibrium and restricted energy-transfer between photosynthetic units. Biophys J 68:2474–2492

Lázar D (1999) Chlorophyll *a* fluorescence induction. BBA—Bioenergetics 1412:1–28

Lázar D, Schansker G (2009) Models of chlorophyll *a* fluorescence transients. In: Laisk A, Nedbal L, Govindjee (eds) Photosynthesis in silico. Advances in photosynthesis and respiration, vol 29. Springer, Dordrecht, pp 85–123

Lemeille S, Rochaix JD (2010) State transitions at the crossroad of thylakoid signalling pathways. Photosynth Res 106:33–46

Mamedov M, Govindjee Nadtochenko V, Semenov A (2015) Primary electron transfer processes in photosynthetic reaction centers from oxygenic organisms. Photosynth Res 125:51–63

Margulis L, Barreno E (2003) Looking at lichens. BioScience 53:776–778

Mathur S, Allakhverdiev SI, Jajoo A (2011) Analysis of high temperature stress on the dynamics of antenna size and reducing side heterogeneity of Photosystem II in wheat leaves (*Triticum aestivum*). Biochim Biophys Acta 1807:22–29

Maxwell K, Johnson GN (2000) Chlorophyll fluorescence—a practical guide. J Exp Bot 51:659–668

Msilini N, Zaghdoudi M, Govindachary S, Lachaal M, Ouerghi Z, Carpentier R (2011) Inhibition of photosynthetic oxygen evolution and electron transfer from the quinone acceptor Q_A^- to Q_B by iron deficiency. Photosynth Res 107:247–256

Munekage Y, Hashimoto M, Miyake C, Tomizawa K, Endo T, Tasaka M, Shikanai T (2004) Cyclic electron flow around photosystem I is essential for photosynthesis. Nature 429:579–582

Okegawa Y, Kobayashi Y, Shikanai T (2010) Physiological links among alternative electron transport pathways that reduce and oxidize plastoquinone in *Arabidopsis*. Plant J 63:458–468

Palmqvist K, Dahlman L, Johnson A, Nash TH III (2008) The carbon economy of lichens. In: Nash TH III (ed) Lichen biology. Cambridge University Press, Cambridge, pp 182–215

Papageorgiou GC, Govindjee (eds) (2004) Chlorophyll fluorescence: a signature of photosynthesis. In: Govindjee (series ed) Advances in photosynthesis and respiration, vol. 19. Kluwer (now Springer), Dordrecht

Pospisil P, Dau H (2000) Chlorophyll fluorescence transients of Photosystem II membrane particles as a tool for studying photosynthetic oxygen evolution. Photosynth Res 65:41–52

Robinson HH, Crofts AR (1983) Kinetics of the oxidation–reduction reactions of the photosystem II quinone acceptor complex, and the pathway for deactivation. FEBS Lett 153:221–226

Rundel PW (1988) Water relations. In: Galun M (ed) Handbook of lichenology. CRC Press, Boca Raton, pp 17–36

Sánchez-Muñoz BA, Aguilar MI, King-Díaz B, Fausto-Rivero J, Lotina-Hennsen B (2012) The sesquiterpenes β-caryophyllene and caryophyllene oxide isolated from *Senecio salignus* act as phytogrowth and photosynthesis inhibitors. Molecules 17:1437–1447

Schansker G, Strasser RJ (2005) Quantification of non-Q(B)-reducing centers in leaves using a far-red pre-illumination. Photosynth Res 84:145–151

Slavov C, Reus M, Holzwarth AR (2013) Two Different Mechanisms cooperate in the desiccation-induced excited state quenching in Parmelia lichen. J Phys Chem 117:11326–11336

Stirbet A, Govindjee G (2011) On the relation between the Kautsky effect (chlorophyll *a* fluorescence induction) and Photosystem II: basics and applications of the OJIP fluorescence transient. J Photochem Photobiol 104:236–257

Stirbet A, Govindjee G (2012) Chlorophyll *a* fluorescence induction: understanding the thermal phase, the J-I-P rise. Photosynth Res 113:15–61

Stirbet A, Govindjee G, Strasser BJ, Strasser RJ (1998) Chlorophyll *a* fluorescence induction in higher plants: modelling and numerical simulation. J Theor Biol 193:131–151

Strasser RJ (1978) The grouping model of plant photosynthesis. In: Akoyunoglou G (ed) Chloroplast development. Elsevier/North Holland, Amsterdam, pp 513–524

Strasser RJ (1981) The grouping model of plant photosynthesis: heterogeneity of photosynthetic units in thylakoids. In: Akoyunoglou G (ed) Photosynthesis III. Structure and molecular organisation of the photosynthetic apparatus, Balaban International Science Services, Philadelphia, pp 727–737

Strasser RJ (1986) Monopartite bipartite tripartite and polypartite models in photosynthesis. Photosynth Res 10:255–276

Strasser RJ, Govindjee G (1991) The Fo and the O-J–I–P fluorescence rise in higher plants and algae. In: Argyroudi-Akoyunoglou JH (ed) Regulation of chloroplast biogenesis. Plenum Press, New York, pp 423–426

Strasser RJ, Govindjee G (1992) On the O-J–I–P fluorescence transients in leaves and D1 mutants of Chlamydomonas reinhardtii. In: Murata N (ed) Research in photosynthesis. Kluwer, Dordrecht, pp 39–42

Strasser RJ, Greppin H (1981) Primary reactions of photochemistry in higher plants. In: Akoyunoglou G (ed) Photosynthesis III. Structure and molecular organisation of the photosynthetic apparatus. Balaban International Science Services, Philadelphia, pp 717–726

Strasser RJ, Stirbet AD (1998) Heterogeneity of Photosystem II probed by the numerically simulated chlorophyll *a* fluorescence rise (O-J-I-P). Math Comput Simul 48:3–9

Strasser RJ, Strasser BJ (1995) Measuring fast fluorescence transients to address environmental questions: the JIP-test. In: Mathis P (ed) Photosynthesis: from light to biosphere. Kluwer, Dordrecht, pp 977–980

Strasser RJ, Tsimilli-Michael M (1998) Activity and heterogeneity of PSII probed in vivo by the chlorophyll *a* fluorescence raise O-(K)-J-I-P. In: Garab G (ed) Photosynthesis: mechanisms and effects, vol V. Kluwer, Dordrecht, pp 4321–4324

Strasser RJ, Tsimilli-Michael M (2001) Structure function relationship in the photosynthetic apparatus: a biophysical approach. In: Pardha-Saradhi P (ed) Biophysical processes in living systems. Science Publishers, Enfield, pp 271–303

Strasser RJ, Srivastava A, Tsimilli-Michael M (2000) The fluorescence transient as a tool to characterize and screen photosynthetic samples. In: Yunus M, Pathre U, Mohantz P (eds) Probing photosynthesis: mechanism, regulation and adaptation. Taylor and Francis, London, pp 443–480

Strasser RJ, Tsimilli-Michael M, Srivastava A (2004) Analysis of the chlorophyll *a* fluorescence transient. In: Papageorgiou GC, Govindjee G (eds) Chlorophyll *a* fluorescence: a signature of photosynthesis. Springer, Dordrecht, pp 321–362

Thach LB, Shapcott A, Schmidt S, Critchley C (2007) The OJIP fast fluorescence rise characterizes *Graptophyllum* species and their stress responses. Photosynth Res 94:423–436

Tóth SZ, Schansker G, Strasser RJ (2005) In intact leaves, the maximum fluorescence level (F_m) is independent of the redox state of the plastoquinone pool: a DCMU-inhibition study. Biochim Biophys Acta 1708:275–282

Tóth SZ, Schansker G, Strasser RJ (2007) A noninvasive assay of the plastoquinone pool redox state based on the OJIP transient. Photosynth Res 93:193–203

Treves H, Raanan H, Finkel OM, Berkowicz SM, Keren N, Shotland Y, Kaplan A (2013) A newly isolated *Chlorella* sp. from desert sand crusts exhibits a unique resistance to excess light intensity. FEMS Microbiol Ecol 86:373–380

Tsimilli-Michael M, Strasser RJ (2013) The energy flux theory 35 years later: formulations and applications. Photosynth Res 117:289–320

Tuba Z, Csintalan Z, Proctor MCF (1996) Photosynthetic responses of a moss, *Tortula ruralis*, ssp. *ruralis*, and the lichens *Cladonia convoluta* and *C. furcata* to water deficit and short periods of desiccation, and their ecophysiological significance: a baseline study at present-day CO_2 concentration. New Phytol 133:353–361

Veerman J, Vasil'ev S, Paton GD, Ramanauskas J, Bruce D (2007) Photoprotection in the lichen *Parmelia sulcata*: the origins of desiccation-induced fluorescence quenching. Plant Physiol 145:997–1005

Velthuys BR (1981) Electron-dependent competition between plastoquinone and inhibitors for binding to Photosystem II. FEBS Lett 126:277–281

Vredenberg WJ, Bulychev AA (2003) Photoelectric effects on chlorophyll fluorescence of photosystem II in vivo. Kinetics in the absence and presence of valinomycin. Bioelectrochemistry 60:87–95

Vredenberg W, Kasalicky V, Durchan M, Prasil O (2006) The chlorophyll *a* fluorescence induction pattern in chloroplasts upon repetitive single turnover excitations: accumulation and function of Q_B-nonreducing centers. Biochim Biophys Acta 1757:173–181

Yamakawa H, Fukushima Y, Itoh S, Heber U (2012) Three different mechanisms of energy dissipation of a desiccation-tolerant moss serve one common purpose: to protect reaction centres against photo-oxidation. J Exp Bot 63:3765–3775